energies

MDPI

Article

Legacy Well Leakage Risk Analysis at the Farnsworth Unit Site

Shaoping Chu [1,*], Hari Viswanathan [1] and Nathan Moodie [2]

[1] Earth and Environmental Sciences Division, Los Alamos National Laboratory, Los Alamos, NM 87545, USA; viswana@lanl.gov
[2] Energy and Geoscience Institute, The University of Utah, Salt Lake City, UT 84108, USA; nathan.moodie@m.cc.utah.edu
* Correspondence: spchu@lanl.gov; Tel.: +1-505-667-9190

Abstract: This paper summarizes the results of the risk analysis and characterization of the CO_2 and brine leakage potential of Farnsworth Unit (FWU) site wells. The study is part of the U.S. DOE's National Risk Assessment Partnership (NRAP) program, which aims to quantitatively evaluate long-term environmental risks under conditions of significant geologic uncertainty and variability. To achieve this, NRAP utilizes risk assessment and computational tools specifically designed to quantify uncertainties and calculate the risk associated with geologic carbon dioxide (CO_2) sequestration. For this study, we have developed a workflow that utilizes physics-based reservoir simulation results as input to perform leakage calculations using NRAP Tools, specifically NRAP-IAM-CS and RROM-Gen. These tools enable us to conduct leakage risk analysis based on ECLIPSE reservoir simulation results and to characterize wellbore leakage at the Farnsworth Unit Site. We analyze the risk of leakage from both individual wells and the entire field under various wellbore integrity distribution scenarios. The results of the risk analysis for the leakage potential of FWU wells indicate that, when compared to the total amount of CO_2 injected, the highest cemented well integrity distribution scenario (FutureGen high flow rate) exhibits approximately 0.01% cumulative CO_2 leakage for a 25-year CO_2 injection duration at the end of a 50-year post-injection monitoring period. In contrast, the highest possible leakage scenario (open well) shows approximately 0.1% cumulative CO_2 leakage over the same time frame.

Keywords: CO_2 storage; leakage risk assessment; reservoir simulation; NRAP tools

check for updates

Citation: Chu, S.; Viswanathan, H.; Moodie, N. Legacy Well Leakage Risk Analysis at the Farnsworth Unit Site. *Energies* **2023**, *16*, 6437. https://doi.org/10.3390/en16186437

Academic Editor: Fabio Montagnaro

Received: 28 July 2023
Revised: 26 August 2023
Accepted: 29 August 2023
Published: 6 September 2023

Copyright: © 2023 by the authors. Licensee MDPI, Basel, Switzerland. This article is an open access article distributed under the terms and conditions of the Creative Commons Attribution (CC BY) license (https://creativecommons.org/licenses/by/4.0/).

1. Introduction

Carbon capture, utilization, and storage (CCUS) in geological reservoirs is among the key strategies being employed to reach mid-century climate targets [1,2]. Phase III of the Southwest Regional Partnership on Carbon Sequestration (SWP) has successfully injected and stored approximately 800,000 metric tons of CO_2 at the Farnsworth Unit (FWU) in northern Texas. A site of active CO_2-enhanced oil recovery (CO_2-EOR) since 2010 [3–5]. The SWP project has demonstrated commercial CCUS field operations focusing on reservoir engineering, monitoring, simulations, and risk assessment to ensure safe and secure sequestration of CO_2. The learnings from the project have contributed to best practices manuals for geologic carbon storage, providing insights and lessons for future CCUS projects.

It has become increasingly important that stakeholders require quantitative assessments of risks to help make decisions related to the effectiveness and management of geologic carbon sequestration sites [6]. To better support the deployment of commercial-scale integrated carbon capture and storage (CCS) projects and provide guidance on strategic monitoring and post-injection site care (PISC) plans, many site-specific pre-feasibility and feasibility studies have been conducted to assess the risk of potential well leakage. White et al. [7] demonstrated this using NRAP tools for risk-based delineation of an Area of Review (AoR) that represents the region that may be affected by the injection of CO_2 and

assessed site-specific leakage risks that might impact the quality of underground sources of drinking water (USDWs). Xiao et al. [8] reviewed leakage risk assessment studies, and pointed out that in most risk assessment studies, abandoned legacy wells with hypothetical open boreholes and/or wellbore failures are assumed as the most likely leakage pathways [9–11].

The NRAP-Open-IAM is a system-level integrated assessment model that was developed by the United States Department of Energy (DOE) for quantitative risk assessment of the geologic sequestration of CO_2 [12,13]. It is built on the CO_2-PENS model structure [14], which was developed with the GoldSim® software framework [15]. The model takes a stochastic approach with Monte-Carlo studies of multiple realizations. Examples of NRAP-IAM-CS applications can be found in Pawar et al., 2016 [13]. For this study, a workflow has been developed to import physics-based reservoir simulator (ECLIPSE®) pressure and CO_2 saturation results into the NRAP integrated assessment toolset.

This manuscript describes the quantitative risk and uncertainty assessment applied to the Farnsworth Unit, a site in north Texas of ongoing CO_2-EOR that has been under study by the Southwest Regional Partnership on Carbon Sequestration (SWP) since 2010 [3,16–21]. The focus of this study was the quantification of the CO_2 and brine leakage potential of legacy wells within the FWU. Geo-cellular models created with characterization data, along with advanced approaches, have been employed to improve the effectiveness of risk quantification [16,22,23]. This manuscript reviews the key conclusions regarding leakage risk and uncertainty assessment and provides insights from the SWP project. This insight can be used to guide future risk assessment applications for other large-scale CCUS projects.

2. Materials and Methods

2.1. NRAP Tools and Integrated Assessment Modeling Approach

Among the NRAP toolset used for this study, the Integrated Assessment Model for Carbon Storage (NRAP-IAM-CS) adopts a stochastic approach in which predictions address uncertainties in storage reservoirs, leakage scenarios, and shallow groundwater impacts. It is derived from detailed physics and chemistry simulation results that are used to train more computationally efficient models, referred to here as reduced-order models (ROMs), for each component of the system. The Reservoir Reduced-Order Model Generator (RROM-Gen) [24] is a utility program for creating reservoir ROM lookup tables to be fed into the NRAP-IAM-CS model. These tools are used in the workflow to import storage reservoir simulator results of pressure and CO_2 saturation as input for the NRAP integrated assessment model (IAM) via RROM-Gen, carry out the CO_2 and brine leakage calculations, and perform risk analysis for the FWU site. FWU site descriptions can be found in Czoski 2014 [16], Ross-Coss et al., 2016 [17], and Xiao et al., 2020 [8].

Figures 1 and 2 show the NRAP-IAM-CS model schematic diagram and domain. Detailed instructions on how to use the model can be found in the NRAP Integrated Assessment Model-Carbon Storage (NRAP-IAM-CS) Tool User's Manual [25].

Figure 3 shows NRAP's approach for rapid prediction of whole-system risk performance. The approach includes the following steps:

A. Divide the system into discrete components;
B. Develop detailed component models that are validated against lab/field data;
C. Develop reduced-order models (ROM) that rapidly reproduce component model predictions;
D. Link ROMs via integrated assessment models (IAMs) to predict system performance and risk; calibrate using lab/field data from NRAP and other sources;
E. Develop strategic monitoring protocols that allow verification of predicted system performance.

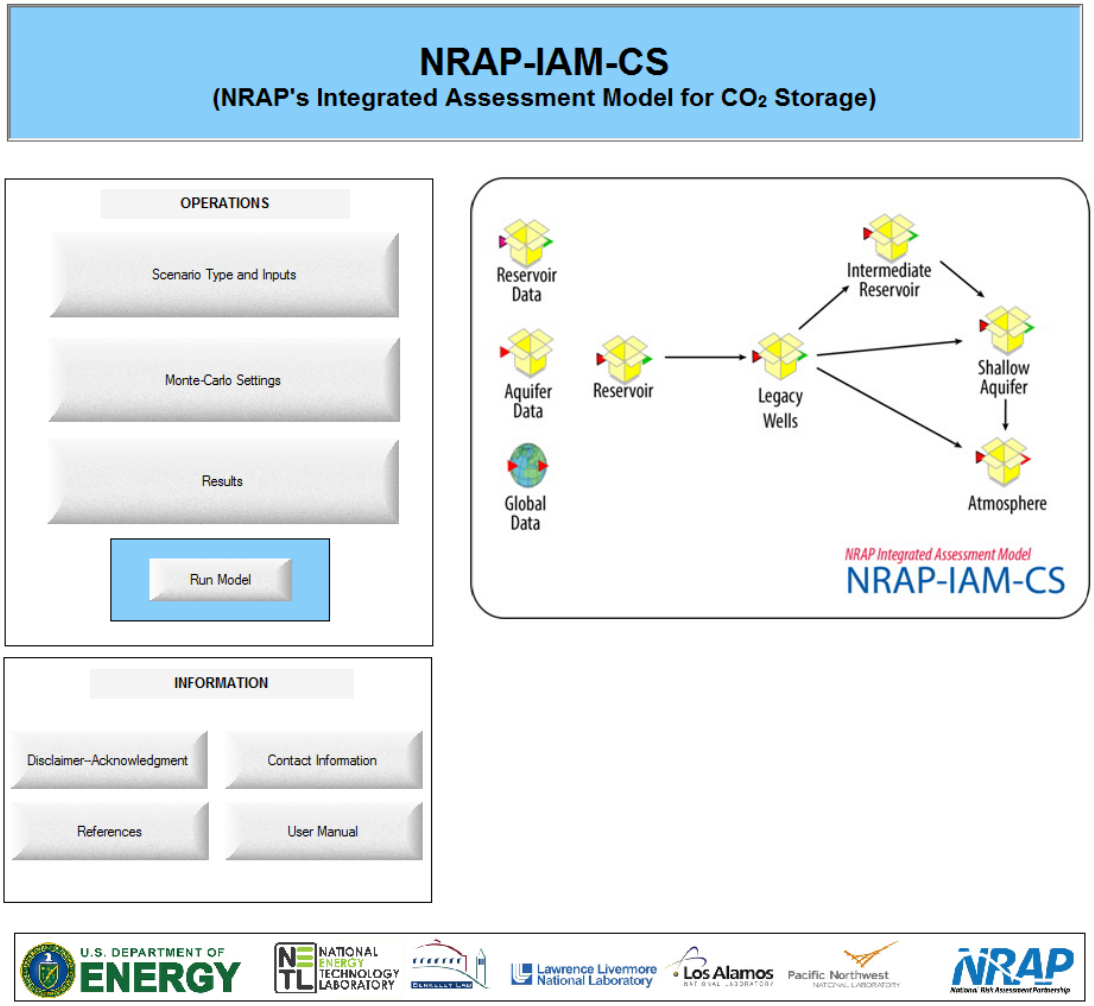

Figure 1. The NRAP-IAM-CS model's schematic diagram shown on top level dashboard.

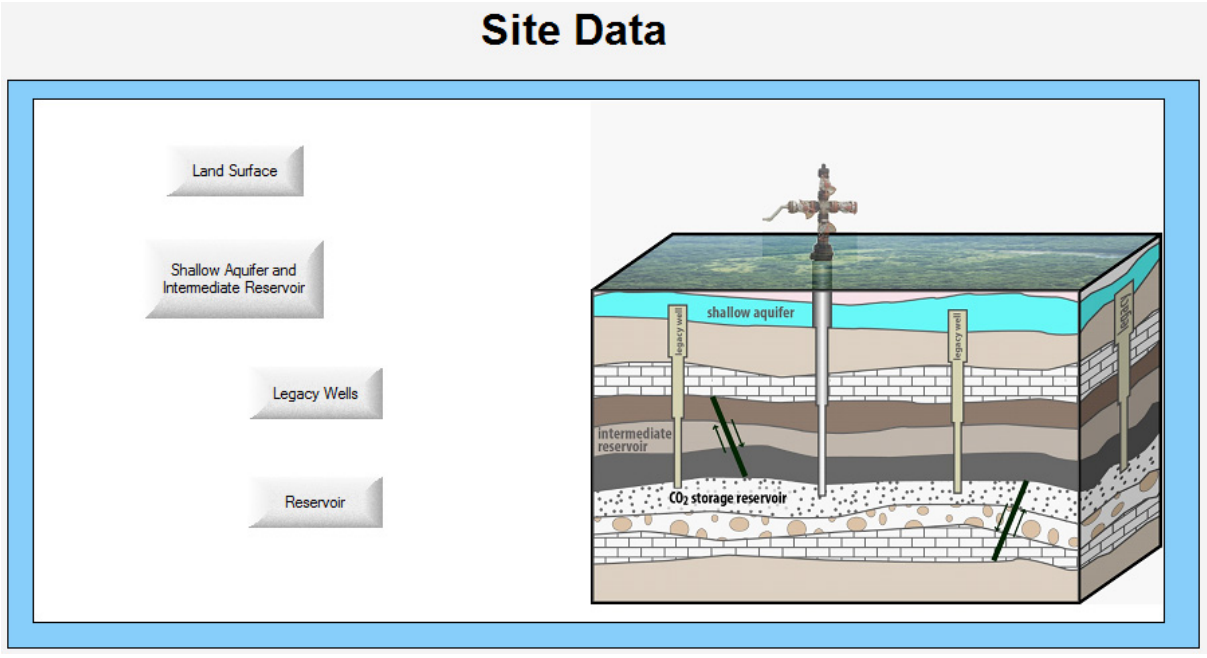

Figure 2. The NRAP-IAM-CS model's domain.

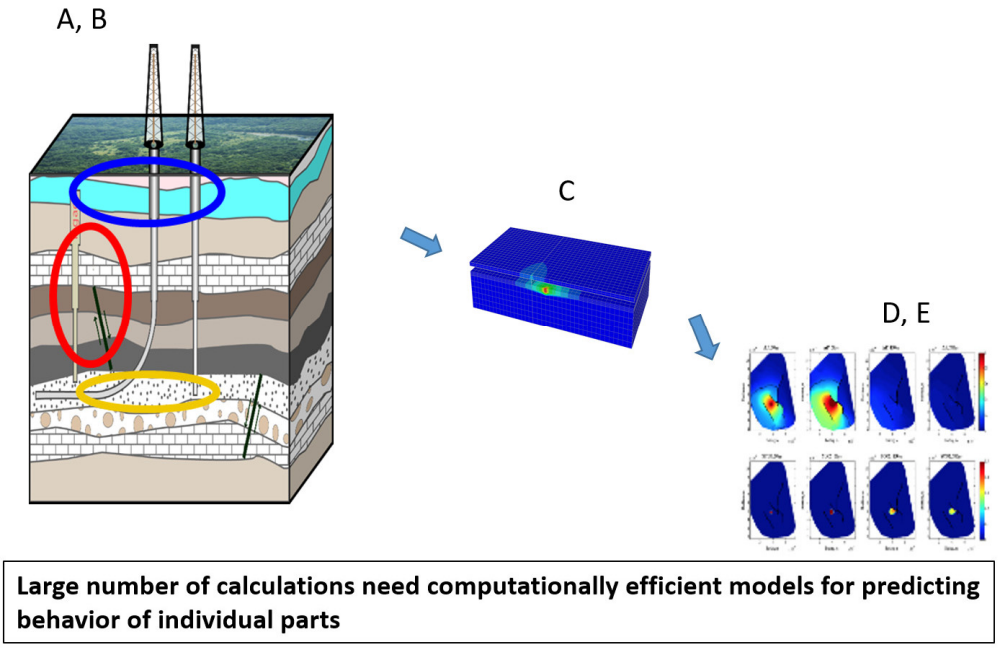

Figure 3. NRAP's approach for rapid prediction of whole-system risk performance.

Applying the NRAP tools (NRAP-IAM-CS, RROM-Gen) to CO_2-EOR operations at the FWU, we conducted a leakage risk analysis using the ECLIPSE reservoir simulation results (for a detailed discussion, refer to Sections 2.2 and 2.3). We selected the pressure and CO_2 saturation results from a comprehensive range of CO_2-EOR reservoir simulation scenarios. Each reservoir scenario represented distinct reservoir conditions resulting from different assignments of relative permeability and capillary pressure aimed at assessing the impact of CO_2 injection volume and fluid mobility. These fields were then converted and input into the NRAP's Integrated Assessment Model to perform risk quantification for CO_2 and brine leakage calculations.

There are three main components of NRAP-IAM-CS used for this study: the storage reservoir, legacy wells, and the shallow groundwater aquifer. The storage reservoir component predicts pressure and saturation changes due to CO_2 injection. For this study, these fields are imported as lookup tables from the ECLIPSE reservoir simulation results. We use the cemented wellbore component and the open wellbore component for legacy well CO_2 and brine leakage calculations.

The NRAP-IAM-CS model is developed using FWU site-specific well locations, stratigraphy, and characterization data following the guidelines described in the NRAP Integrated Assessment Model-Carbon Storage (NRAP-IAM-CS) Tool User's Manual [25]. Multi-realization probabilistic simulations are carried out, sampling various reservoir scenarios and different wellbore integrity distributions. Detailed analysis and quantification of wellbore CO_2 and brine leakage are performed.

To address the uncertainties regarding wellbore leakage and the limited availability of wellbore permeability data at FWU, an investigation into the influence of wellbore integrity on leakage was undertaken. NRAP's Integrated Assessment Model was configured for simulating and assessing CO_2 and brine leakage across various scenarios of wellbore integrity and permeability. Numerous probability distribution models for wellbore effective permeability were examined, drawing from Carey's 2017 study [26] on wellbore effective permeability in areas like Alberta, the Gulf of Mexico, and FutureGen's low/high flow rate conditions. These effective permeability distributions have been consolidated in Table 1. It is important to note that the last two categories—a cemented well with an extremely high fixed permeability of 5×10^{-11} (which is the upper limit allowed in the NRAP-IAM-CS model) and an open well—are hypothetical situations included here to facilitate a conservative worst-case scenario assessment.

Table 1. Wellbore integrity permeability distribution.

Distribution Model	Type	Low End (m^2)	Midrange (m^2)	High End (m^2)
Alberta	Uniform	95.4% of wells 10^{-20}	4.4% of wells 10^{-17}~10^{-14}	0.2% of wells 10^{-13}~10^{-12}
Gulf of Mexico	Uniform	88% of wells 10^{-20}	11.4% of wells 10^{-17}~10^{-14}	0.6% of wells 10^{-13}~10^{-12}
FutureGen low flow rate	Log-normal	90% of wells 10^{-20} (mean)		10% of wells 10^{-17}~10^{-15} (mean)
FutureGen high flow rate	Log-normal	90% of wells 10^{-20}~10^{-18} (mean)		10% of wells 10^{-15}~10^{-13} (mean)
Cemented Well (hypothetically assume all wells with very high fixed permeability)				100% of wells 5×10^{-11}
Open Well (hypothetical)				100% of wells

As the first step in this study, a preliminary IAM simulation with a fixed wellbore permeability of 5×10^{-11} m^2 is performed to test out the workflow. The simulation duration is set up to be 75 years, with CO_2 injection lasting 25 years and a post-injection monitoring period of 50 years. Figure 4 shows the mean cumulative CO_2 and brine leakage for a combination of storage reservoir scenarios. The CO_2 leak rate increases with injection; once injection stopped, the leak rate plateaued, resulting in a curved cumulative CO_2 leakage time series, while the brine leak rate did not vary significantly over time, corresponding to a linear cumulative leakage. Detailed analysis of each scenario and quantification of wellbore leakage uncertainties are described in Section 3, with several aspects of analysis performed: quantification of CO_2 and brine leakage with various reservoir scenarios (Section 3.1), impact of different wellbore integrity conditions (Section 3.2), open well scenario (Section 3.3), and contribution from individual wells to overall leakage (Sections 3.4 and 3.5).

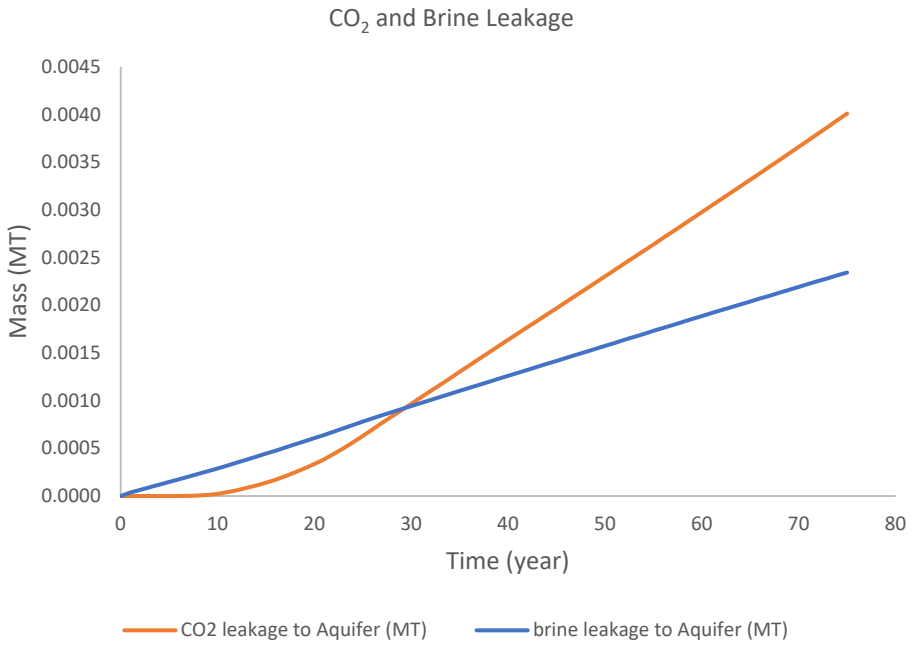

Figure 4. Mean cumulative CO_2 and brine leakage for a combination of reservoir scenarios.

2.2. Reservoir Model of FWU

We performed multiple numerical simulations of CO_2-EOR operations to analyze the impact of various reservoir permutation scenarios. A history-matched numerical model was developed by the SWP from the latest characterization data, covering an area of 31 km^2 centered on the active western half of the field and encompassing the entire Morrow Formation [17,22,23].

The simulation model is 5.52 km east-west and 5.63 km north-south, discretized into 121 × 123 cells. Each cell has an average area of 2082 m^2. The vertical domain (z) is discretized into 19 layers, including six layers in the Morrow Shale, six layers in the Morrow B Sandstone, four layers in the underlying Morrow D unit, and three layers at the bottom of the Morrow Formation. The model includes both the overlying Morrow Shale and the underlying section of the Morrow Formation, resulting in a total of 282,777 active cells in the model. The overlying Thirteen Finger Limestone was not included in the model as it is assumed to have negligible dynamic behavior due to FWU operations [22,23,27].

All simulation permutations were developed using the same underlying numerical model, including porosity and permeability distribution, fluid model, injection schedule, and initial conditions. The model incorporates the latest characterization data from the FWU, including updated well logs and 3D porosity and permeability maps. Porosity from 25 wells and permeability from 14 wells were upscaled to the numerical model grid. Stochastic methods are then employed to distribute the porosity and permeability across the simulation grid. For a detailed description of methods and assumptions used in the numerical model, see Moodie et al., 2019 [23] and Moodie, Ampomah, Heath, et al., 2021 [27].

The CO_2 injection schedule for the numerical simulations was consistent across all the presented simulation cases. The simulation duration spans 75 years, with CO_2 injection taking place during the first 25 years, followed by a post-injection monitoring period of 50 years. The injection schedule has been designed to mimic the potential future CO_2-EOR operations at the FWU, with the initial period receiving an unlimited amount of CO_2, including any recycled CO_2. Post-2016, the availability of "new" CO_2 in the field is gradually reduced, and more reliance is placed on recycled CO_2 to meet targets. CO_2 injection ceases by 2035, which aligns with the anticipated end of the field's lifetime. For specific details of the injection schedule, see Table 2.

Table 2. Injection schedule for numerical simulations.

Injection Period	Injection Fluid
2010–2016	Unlimited CO_2 + recycled CO_2
2016–2024	560 MT/day CO_2 + recycled CO_2
2024–2026	448 MT/day CO_2 + recycled CO_2
2026–2028	392 MT/day CO_2 + recycled CO_2
2028–2030	336 MT/day CO_2 + recycled CO_2
2030–2035	Recycled CO_2 only
2035–2085	Post injection monitoring period

2.3. Reservoir Model Scenarios

To assess potential well leakage at the FWU, we conducted 17 simulation permutations categorized into two main groups: (1) ten simulation cases with a single relative permeability and capillary pressure relationship assigned homogeneously across the model domain, and (2) seven simulation cases with multiple relative permeability and capillary pressure relationships assigned heterogeneously by hydrostratigraphic unit (Table 3). For a comprehensive explanation of the method and assumptions used to assign relative permeability and capillary pressure by hydrostratigraphic unit, see Moodie et al., 2019 [23] and Moodie, Ampomah, Heath, et al., 2021 [27].

Table 3. The numerical simulation models used in the analysis.

Base Model	- 1 case: BaseCase - Legacy relative permeability curve homogeneously assigned - No capillary pressure assigned
Linear model	- 2 cases: Linear and LinearwPc - Linear relative permeability curve homogeneously assigned [both cases] - Capillary pressure assigned homogeneously [LinearwPc] - No capillary pressure assigned [Linear]
Morrow1 Model	- 2 cases: Morrow1 and Morrow1wPc - Laboratory measured relative permeability curve assigned homogenously [both cases] - Capillary pressure curve assigned homogeneously [Morrow1wPc] - No capillary pressure assigned [Morrow1]
Hydrostratigraphic Region 1 Model	- 2 cases: HS1wPc and HS1noPc - 5 relative permeability curves assigned heterogeneously by hydrostratigraphic unit [both case] - 5 capillary pressure curves assigned heterogeneously by hydrostratigraphic unit [HS1wPc] - No capillary pressure assigned [HS1noPc]
Hydrostratigraphic Region 2 Model	- 2 cases: HS2wPc and HS2noPc - 5 relative permeability curves assigned heterogeneously by hydrostratigraphic unit [both cases] - 5 capillary pressure curves assigned heterogeneously by hydrostratigraphic unit [HS2wPc] - No capillary pressure assigned [HS2noPc]
Hydrostratigraphic Region 3 Model	- 2 cases: HS3wPc and HS3noPc - 5 relative permeability curves assigned heterogeneously by hydrostratigraphic unit [both curves] - 5 capillary pressure curves assigned heterogeneously by hydrostratigraphic unit [HS3wPc] - No capillary pressure assigned [HS3noPc]
Hydrostratigraphic Region 4 Model	- 6 cases: HS4wPc, HS4wHSU1-2Pc, HS4wHSU3-4Pc, HS4wHSU5Pc, HS4wHSU6Pc, and HS4wHSU7-8Pc - 1 relative permeability curve assigned homogeneously [all cases] - 5 capillary pressure curves assigned heterogeneously corresponding to each hydrostratigraphic unit [HS4wPc] - 1 capillary pressure curve from each hydrostratigraphic unit homogeneously assigned [HS4wHSU1-2Pc through HS4wHSU7-8Pc]

The CO_2 saturation and reservoir pressure results were extracted and converted to the required format using RROM-Gen before being applied to the NRAP-IAM-CS tool. It can be seen from Table 4 that the assigned relative permeability and capillary pressure can significantly influence the volume of CO_2 that can be injected, affecting its distribution in

the reservoir and the potential for leakage. In Figure 5, we show the locations of the wells used in the NRAP-IAM-CS model. This includes 21 CO_2 injection wells (represented by red dots) and 31 legacy wells considered potential pathways for leakage (shown as blue dots). An example of the pressure distribution and CO_2 saturation after processing the numerical simulation results through RROM-Gen is illustrated in Figure 6.

Table 4. Total CO_2 injected in each reservoir simulation permutation.

Total Mass of CO_2 Injected (tons)			
Homogeneous Cases		**Heterogeneous Cases**	
Base Model	9,496,675	HS1wPc	9,240,643
Morrow1	9,590,256	HS1noPc	8,459,803
Morrow1wPc	10,256,219	HS2wPc	9,202,484
Linear	9,613,866	HS2noPc	8,370,725
LinearwPc	10,157,328	HS3wPc	8,859,159
HS4wHSU1-2Pc	9,426,994	HS3noPc	8,507,114
HS4wHSU3-4Pc	8,988,384	HS4wPc	10,065,672
HS4wHSU5Pc	8,988,394		
HS4wHSU6Pc	9,426,962		
HS4wHSU7-8Pc	9,386,476		

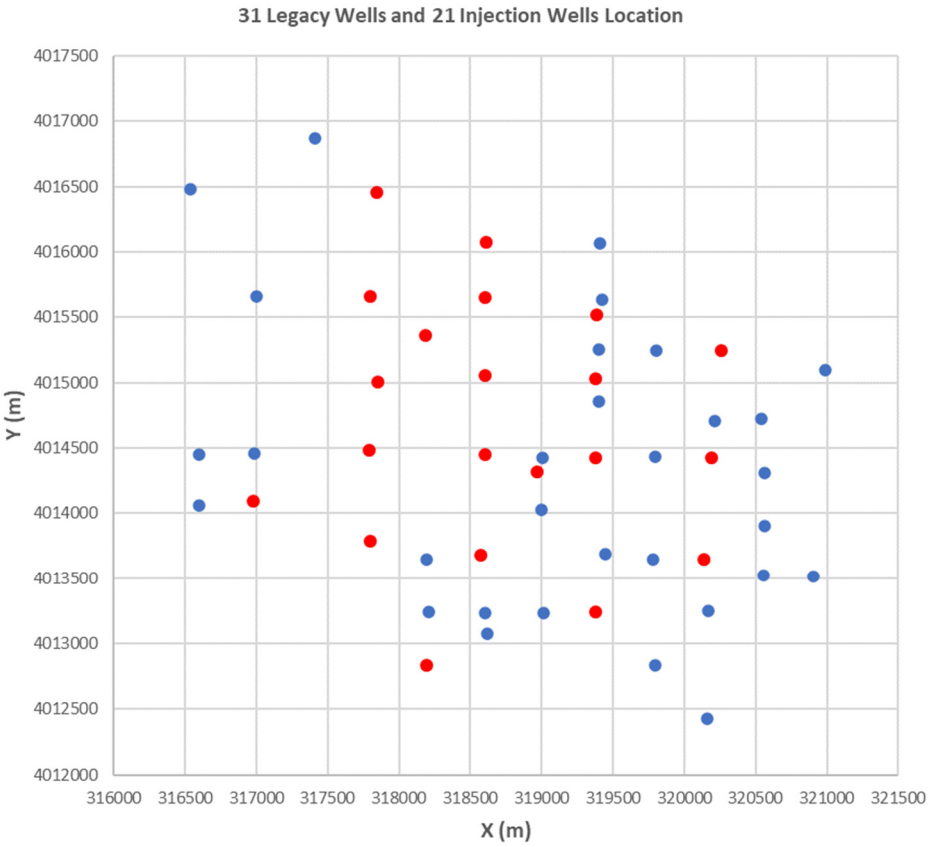

Figure 5. NRAP-IAM-CS model simulation well location for the FWU site. Red dots represent CO_2 injection wells, and blue dots represent potential leakage legacy wells. Numerical values (1 to 31) correspond to successive legacy wells (not marked on this figure).

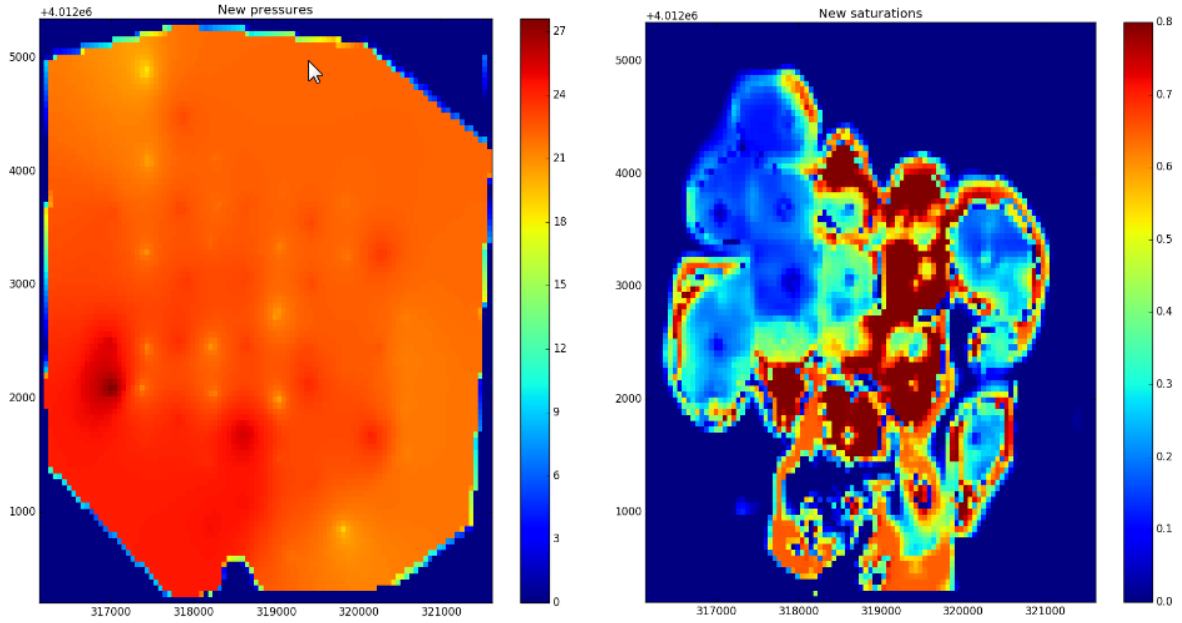

Figure 6. RROM-Gen Response Surface from PETREL-ECLIPSE Reservoir Process Model, as shown in (**a**) (reservoir pressure, left panel) and (**b**) (CO_2 saturation, right panel). The color bar legend shows reservoir pressure ranging from around 18 to 27 MPa and CO_2 saturation ranging from 0 to 80%.

3. Results and Discussion

3.1. NRAP-IAM-CS Quantification of CO_2 and Brine Leakage

NRAP tools are applied for risk quantification of wellbore leakage that covers the full parameter range of reservoir simulations at the Farnsworth Unit Site. Multi-realization probabilistic simulations of CO_2 and brine leakage were carried out, and the impact of various reservoir scenarios and wellbore integrity distribution scenarios is analyzed. Simulations are set up for a CO_2 injection duration of 25 years with a 50-year post-injection monitoring period. Figures 7 and 8 show the cumulative CO_2 and brine leakage to the groundwater aquifer for different reservoir scenarios with a fixed wellbore permeability of 5×10^{-11} m^2.

Figure 7a,b shows simulations with six reservoir category scenarios picked from Table 3 to illustrate the impact of assigned relative permeability and capillary pressure. Some scenarios allow greater fluid movement across the widest saturation range and more leakage (e.g., linear scenario, green line in Figure 7a), while other scenarios with capillary pressure added show greatly reduced fluid mobility (e.g., HS2wPc scenario, yellow line in Figure 7a).

The 11 categories shown in Figure 8a,b are chosen over various parameter scenarios to represent the more complex site condition and account for uncertainties associated with FWU site data. Note that all simulation results presented in this study from Figure 8 on are all based on these 11-category reservoir scenarios.

Analysis shows that relative permeability and capillary pressure assignment are the largest controls on fluid flow; CO_2 leakages are more sensitive to the variation in the assignment, while brine leakages are less affected.

Linear (green line): Relative permeability curve homogeneously assigned with no capillary pressure; allow greatest fluid mobility across the widest saturation range.

HS2wPc (yellow line): Five relative permeability curves and five associated capillary pressure curves are heterogeneously assigned; capillary pressure reduces fluid mobility.

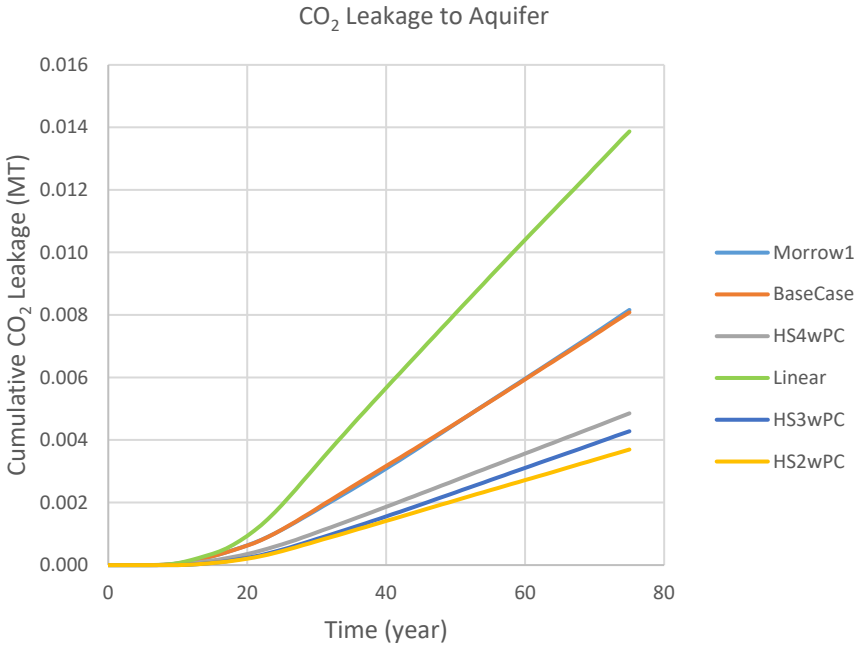

(**a**)

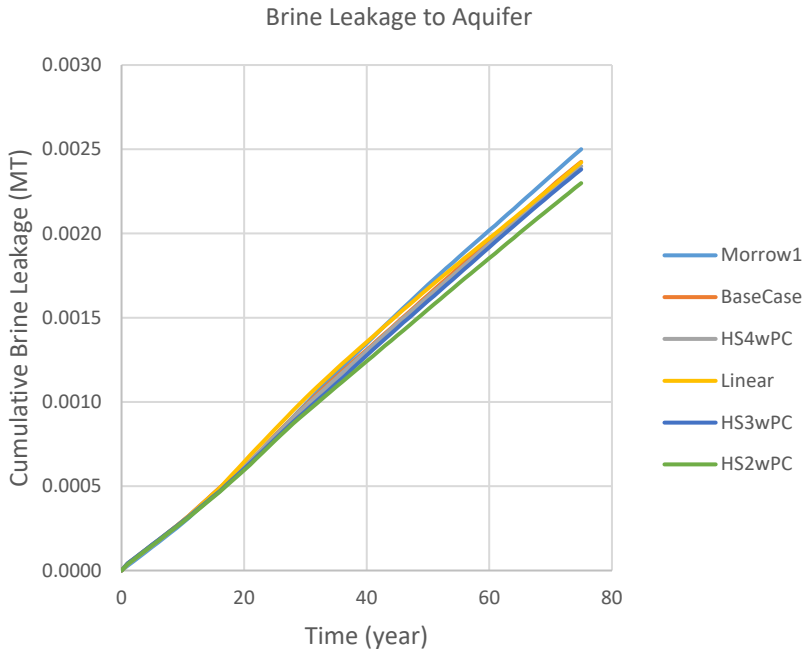

(**b**)

Figure 7. (**a**) Cumulative CO_2 leakage to the groundwater aquifer for a selected group of six reservoir category scenarios shown in Table 4. (**b**) Cumulative brine leakage to the groundwater aquifer for a selected group of six reservoir category scenarios shown in Table 4.

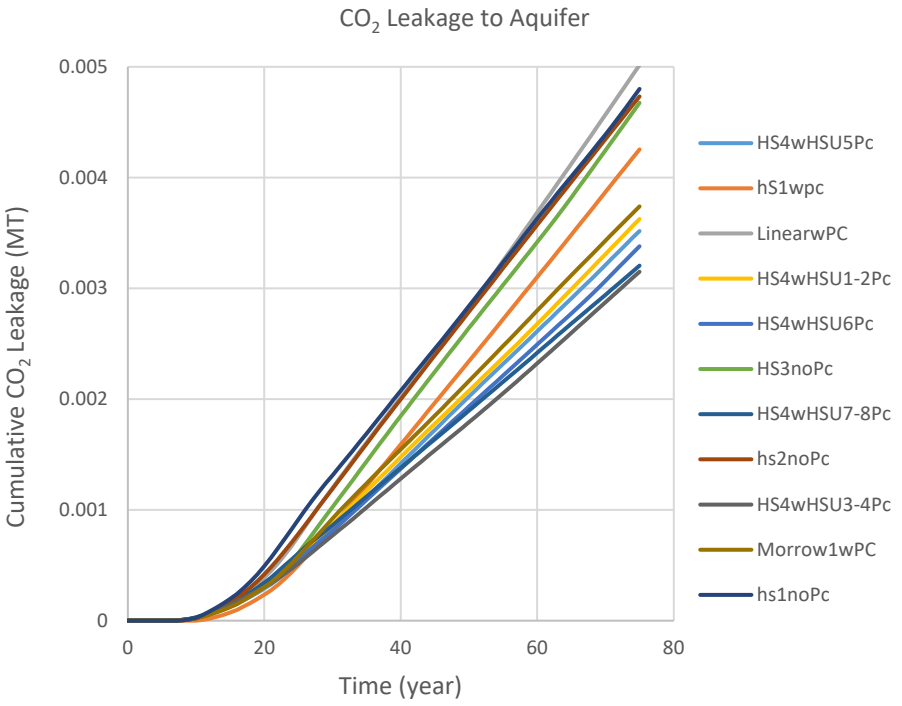

(**a**)

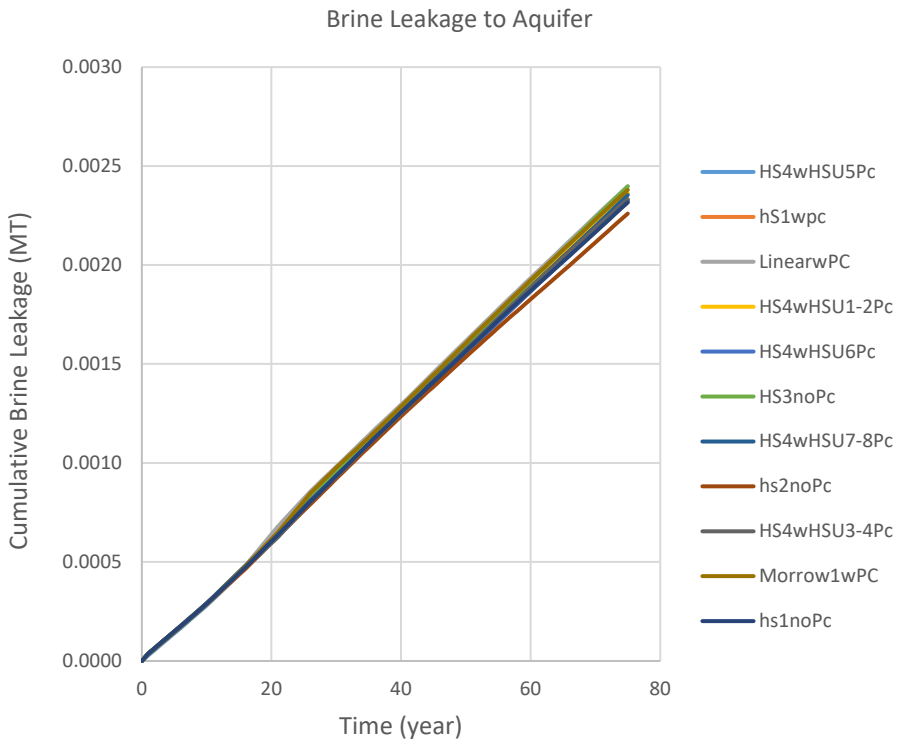

(**b**)

Figure 8. (**a**) Cumulative CO_2 leakage to the groundwater aquifer for a group of 11 reservoir category scenarios shown in Table 4. (**b**) Cumulative brine leakage to the groundwater aquifer for a group of 11 reservoir category scenarios shown in Table 4.

3.2. Impact of Various Wellbore Integrity Distribution on Leakage

For each wellbore permeability distribution scenario, 1000-realization probabilistic simulations are carried out, sampling among 11 reservoir permutations. Among the four wellbore integrity distributions listed in Table 1, the FutureGen high flow rate model shows the highest permeability distribution overall and therefore has the fastest leaking potential, while Alberta shows the lowest permeability distribution overall, which may lead to the slowest leaking potential for CO_2 and brine leakage.

Figures 9 and 10 show the mean cumulative CO_2 and brine leakages to the groundwater aquifer for different cemented wellbore permeability scenarios, respectively. A hypothetically fixed wellbore permeability of 5×10^{-11} m^2 scenario shows the highest mean cumulative CO_2 and brine leakage. FutureGen's high flow rate model has the highest permeability distribution overall, which leads to the highest leakage among well integrity distribution scenarios. Alberta has the lowest permeability distribution overall, which leads to the slowest CO_2 and brine leakage.

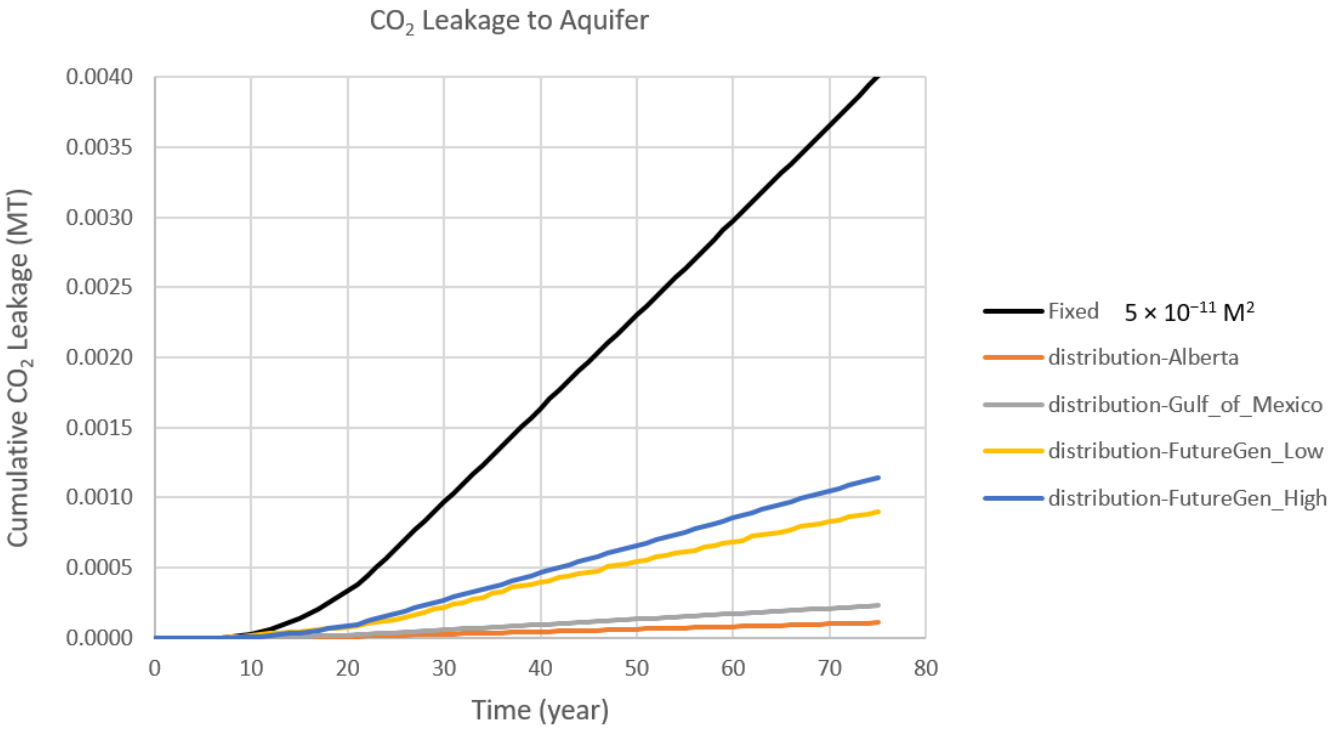

Figure 9. Mean cumulative CO_2 leakages to the groundwater aquifer for different wellbore permeability scenarios.

Compared to the total amount of CO_2 injected, the highest well permeability distribution scenario (FutureGen high flow rate) shows ~0.01% cumulative CO_2 leakage at the end of the 50-year post-injection monitoring period.

3.3. Open Well Leakage Scenario

To check on the largest possible CO_2 and brine leakage in the hypothetically open well condition, we performed CO_2 and brine leakage calculations for the open well scenario. Comparing with cemented wellbore permeability distribution scenarios (Table 4), the open well case (Figures 11 and 12) shows several orders of magnitude increases for CO_2 and brine leakage, starting early, a few years after CO_2 injection started, and then flattening out at around year 12. CO_2 and brine leak very fast through an open well, and leak all CO_2 and brine at the well location quickly.

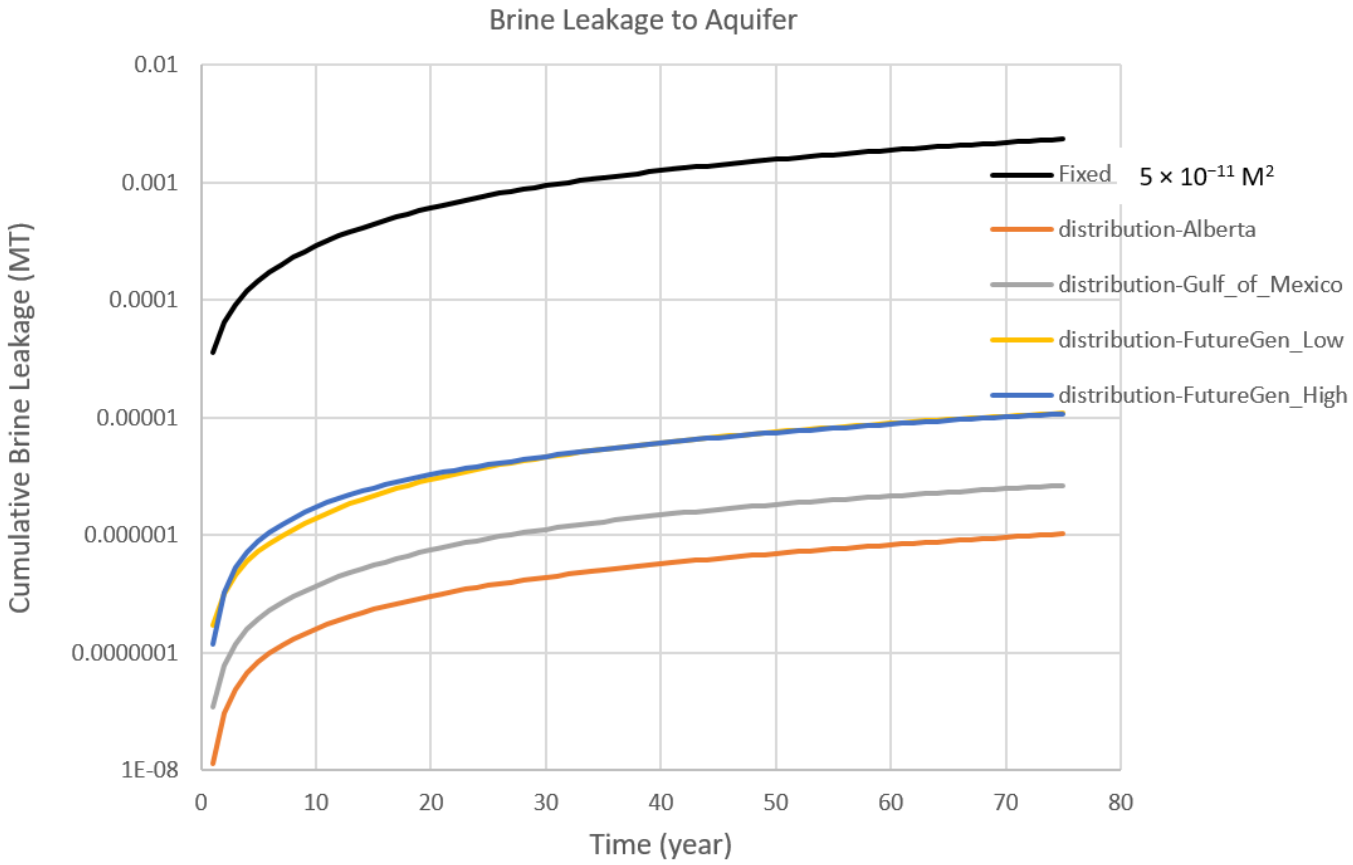

Figure 10. Mean cumulative brine leakages to the groundwater aquifer for different wellbore permeability scenarios.

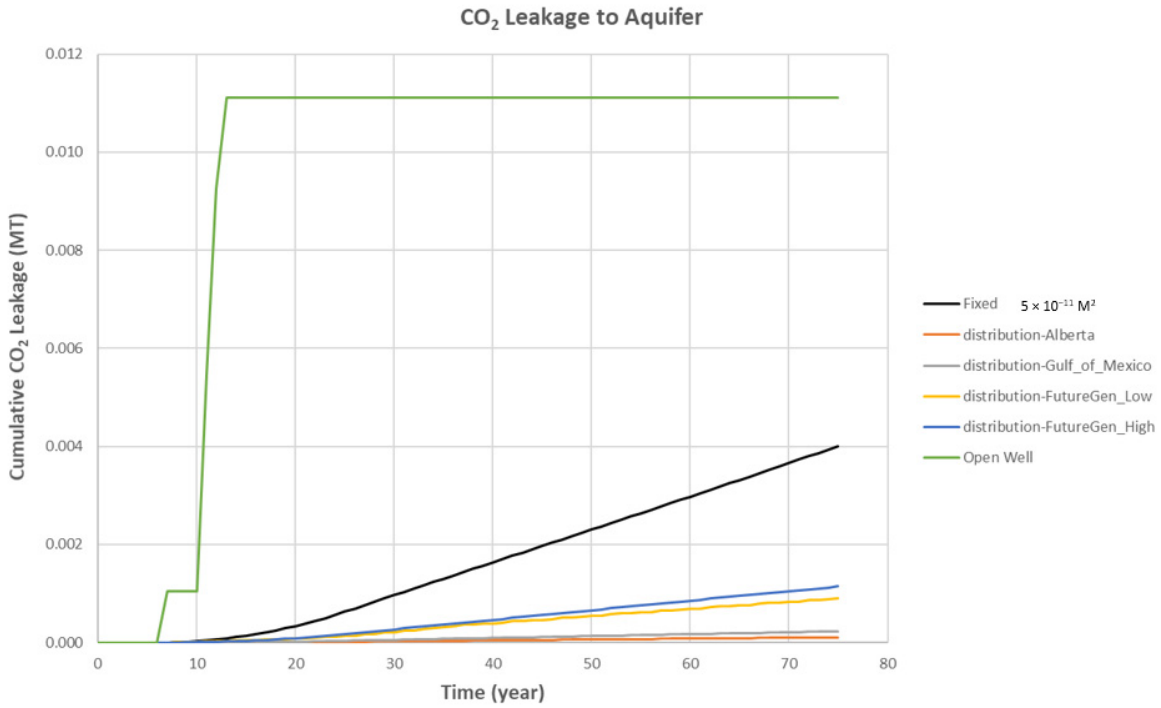

Figure 11. Mean cumulative CO_2 leakage to the groundwater aquifer for different wellbore permeability distributions.

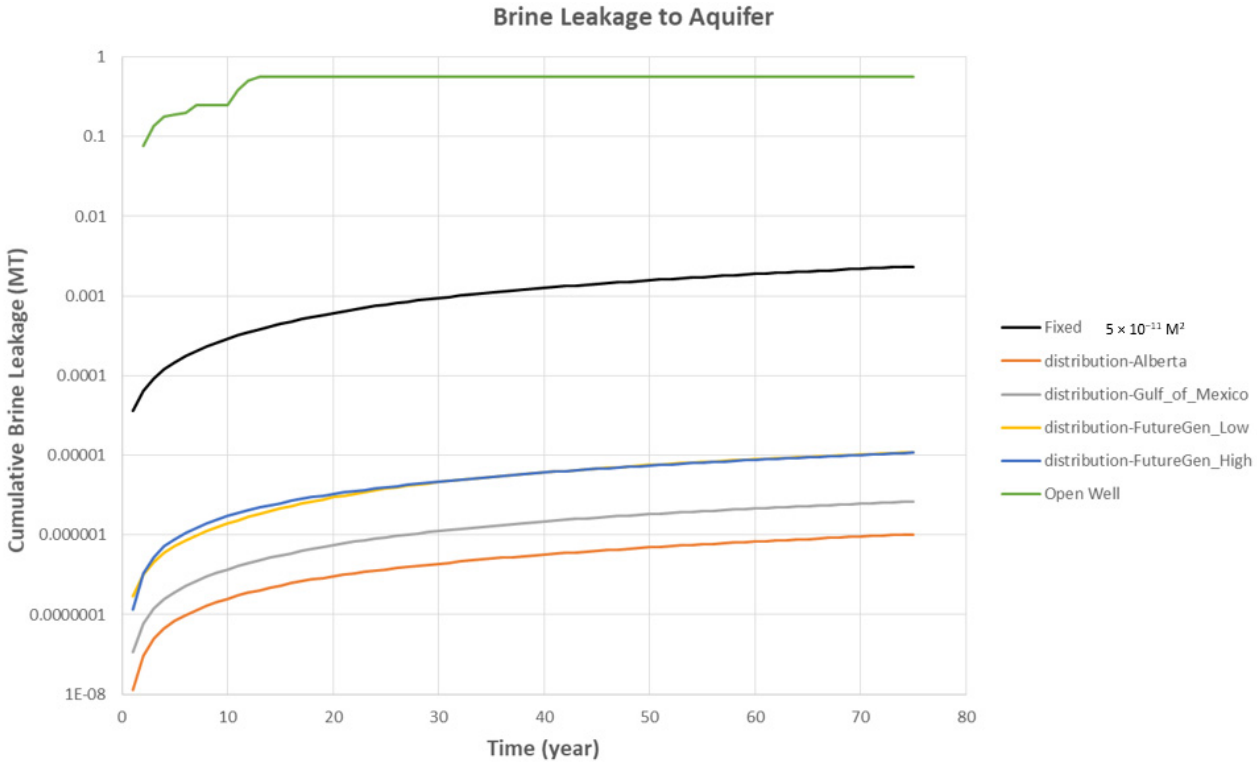

Figure 12. Mean cumulative brine leakage to the groundwater aquifer for different wellbore permeability distributions.

Compared to the total amount of CO_2 injected (about 10 million tons for each permutation scenario), the hypothetical highest possible leakage scenario (open well) shows ~0.1% cumulative CO_2 leakage at the end of the 50-year post-injection monitoring period.

3.4. Individual Well Leakage Analysis—Open Well Scenario

CO_2 and brine leakage calculations are performed in hypothetically open well conditions for each individual well of 31 potential leaking legacy wells to check on each well's contribution towards overall leakage. The simulations were carried out for each legacy well shown in Figure 13 (blue dot).

The simulation results for all 31 legacy wells with a hypothetical open well scenario show that only two legacy wells (well #7 and well #15) have CO_2 leakage to the groundwater aquifer. All legacy wells show brine leakage, but only the two wells with CO_2 leakage (#7 and #15) show a higher level of brine leakage. Well #7 shows the highest cumulative CO_2 and brine leakage.

The analysis for a list of representative legacy wells is summarized in Table 5. Table 5 lists the representative legacy well location, mean cumulative CO_2 and brine leakages to the groundwater aquifer at the end of the 50-year post-injection monitoring period, and also the relative distance of the legacy well from a nearby injection well (i.e., closer or far away from the nearby injection well).

Figure 14 shows the wellbore pressure for the selected legacy wells. It shows wells #7 and #15 have higher wellbore pressure during the time from year 10 to year 25, with well #7 showing the generally highest pressure during this time period. Figure 15 shows that well #15 displays much higher CO_2 saturation, wells #6 and #7 show lower CO_2 saturation, and wells #11 and #22 show an order of magnitude lower amount of CO_2 saturation compared to well #15.

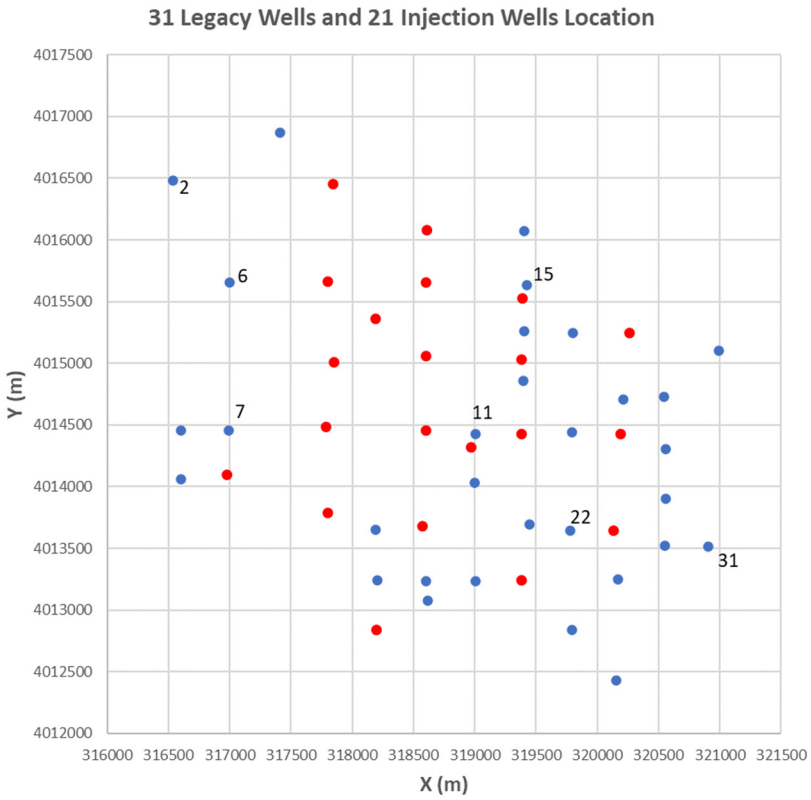

Figure 13. 31 potential leakage legacy well locations (blue dots) and 21 CO_2 injection well locations (red dots). A few representative legacy wells are marked with well numbers.

Table 5. Representative legacy well locations, relative distance to nearby injection wells, and cumulative CO_2 and brine leakage to the groundwater aquifer at the end of the 50-year post-injection monitoring period.

Well #	Relative Distance to Nearby Injection Well	Distance (m) to Nearby Injection Well	Well Coordinate X (m)	Well Coordinate Y (m)	CO_2 Leakage (MT)	Brine Leakage (MT)
7	close	367	316,988	4,014,458	0.01005	0.3345
15	closer	121	319,426	4,015,635	0.001053	0.04434
11	closest	112	319,003	4,014,425	0	0.002614
22	In the middle of Injection wells	360	319,780	4,013,646	0	0.002459
31	far	775	320,905	4,013,513	0	0.002763
6	farther	801	317,001	4,015,657	0	0.02046
2	farthest	1310	316,534	4,016,479	0	0.0136

Figures 16 and 17 show the cumulative CO_2 and brine leakage to the groundwater aquifer from the selected wells. Well #7 displays the highest cumulative CO_2 and brine leakage to the groundwater aquifer. For brine leakage, well #7 displays the highest amount of cumulative leakage, followed by well #15, then well #6, and then wells #11 and #22. CO_2 and brine leak very fast through an open well, and leak all CO_2 and brine at the well location quickly.

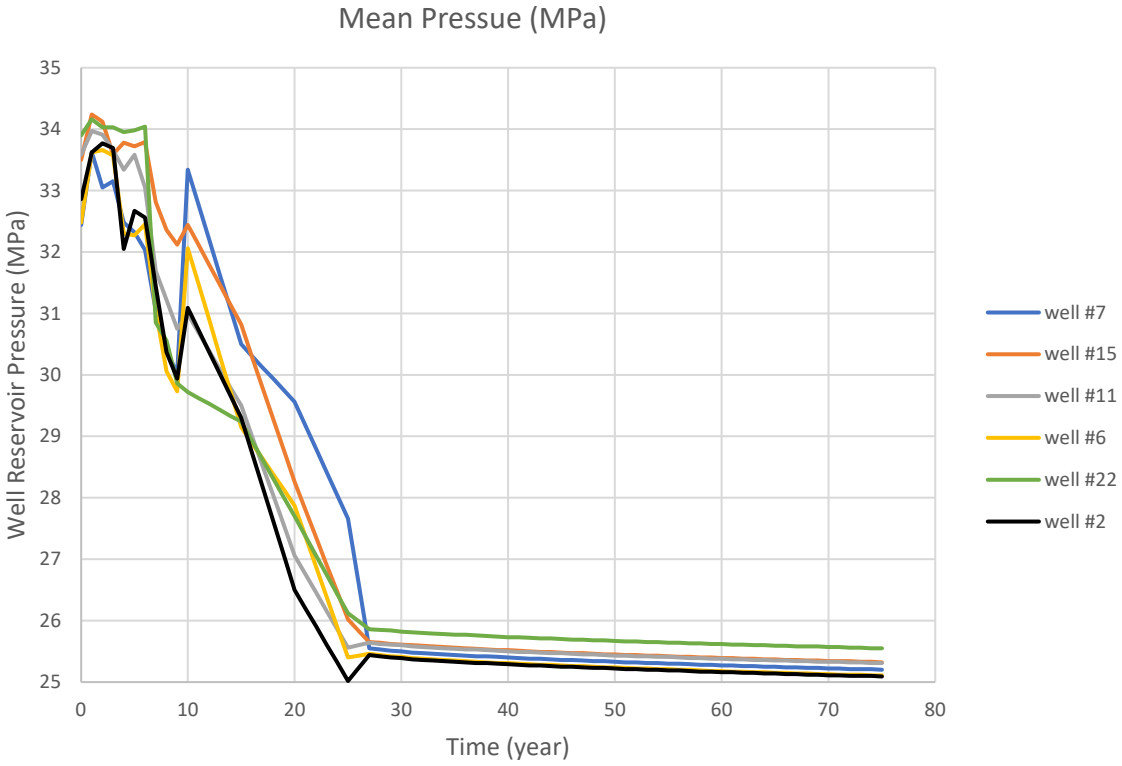

Figure 14. Bottom-hole pressure for the selected legacy wells.

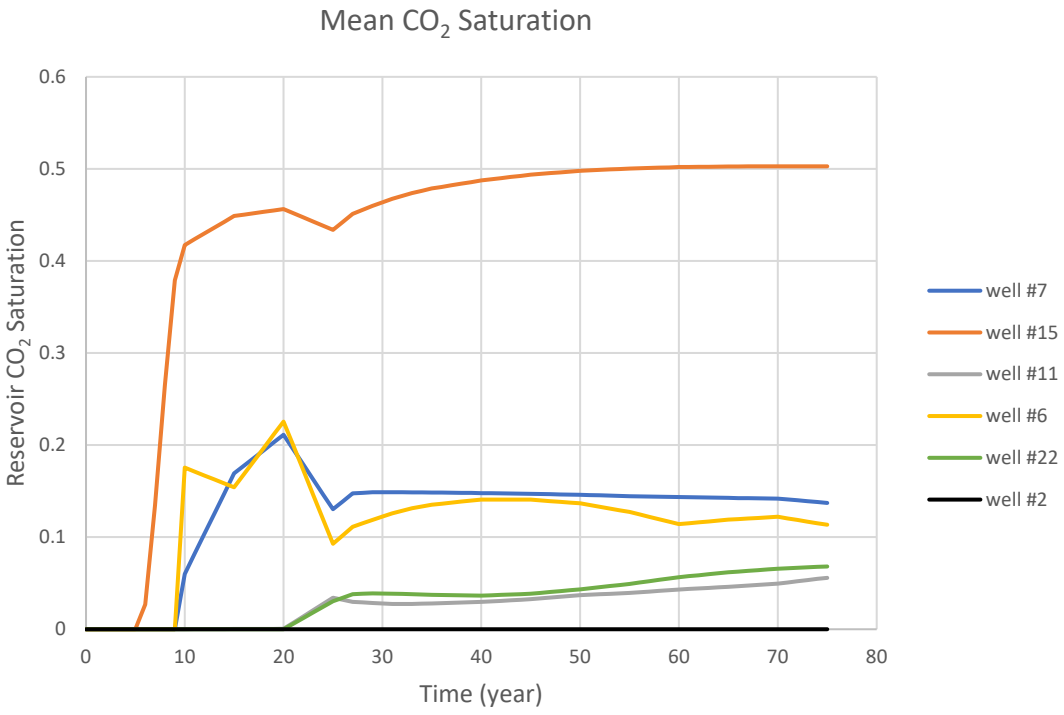

Figure 15. Reservoir CO_2 saturation for selected legacy wells.

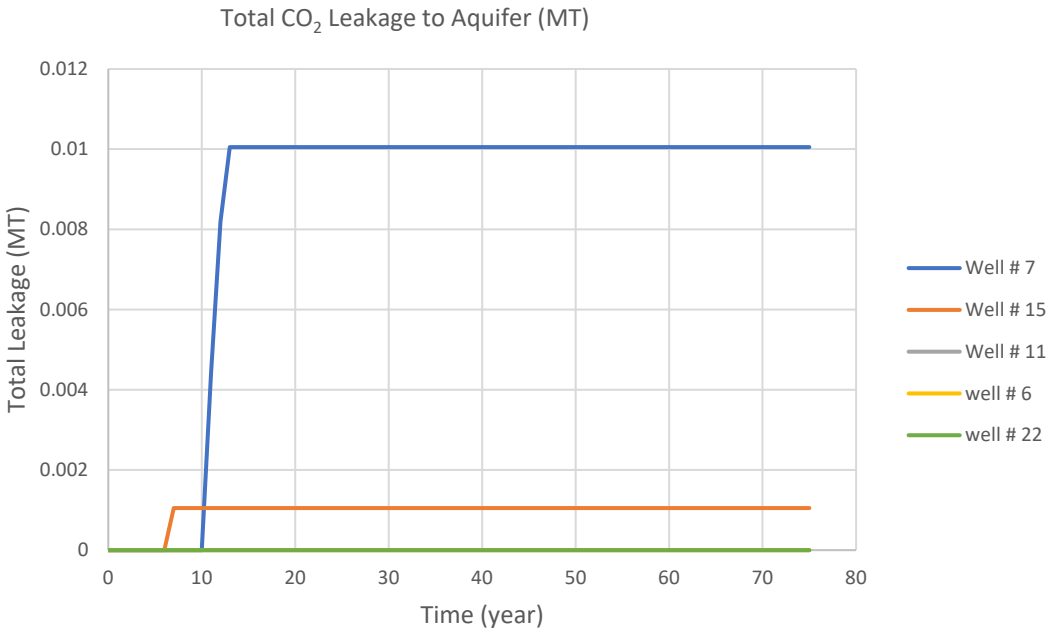

Figure 16. Total cumulative CO_2 leakage to the groundwater aquifer for selected legacy wells in a hypothetical open-well scenario. Leakage from wells #6, 11 and 22 are zero.

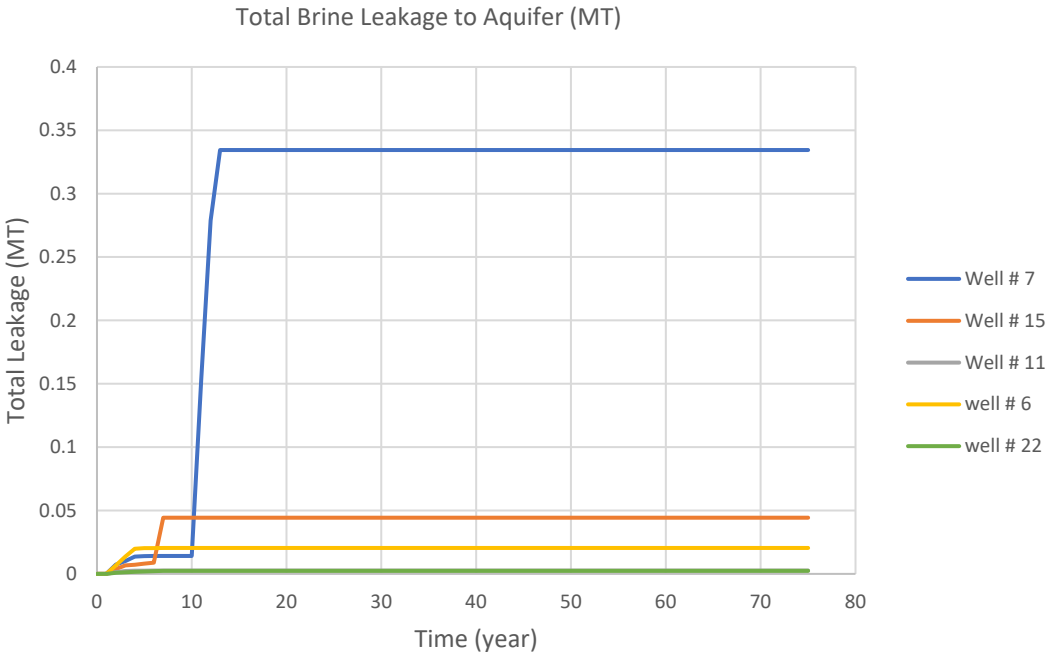

Figure 17. Mean cumulative brine leakage to the groundwater aquifer for selected legacy wells in a hypothetical open-well scenario. Leakage from wells # 11 and 22 are an order of magnitude smaller.

For open well scenario individual well analysis, the situation with multiple injection wells and legacy wells mingled together seems to complicate the analysis in terms of the impact of wellbore pressure, CO_2 saturation, and the distance between a legacy well and a nearby injection well on the potential legacy well CO_2 and brine leakage. For example, well #6 is farther away from a nearby injection well compared to well #7, but it shows about the same level of CO_2 saturation compared to well #7, and it does not show any CO_2 leakage. Well #11 is a legacy well that is the closest to a nearby injection well; however, it does not show CO_2 leakage either. Well #15 shows the highest level of CO_2 saturation, but it has less

CO_2 leakage compared to well #7, which has a lower level of CO_2 saturation but generally higher wellbore pressure during the time period of year 10 to year 25.

3.5. Individual Well Leakage Analysis—Cemented Well Scenario

To check on each well's contribution towards overall leakage CO_2 and brine leakage, analysis is also carried out for cemented wellbore settings. This section describes calculations for individual wells of 31 potential leaking legacy wells at the FWU site with the highest possible effective wellbore permeability (5×10^{-11} m^2) allowed in the NRAP integrated assessment model (NRAP-IAM-CS) as a conservative assessment for cemented wellbore potential leakage risk. According to wellbore permeability distribution data from Carey 2017 [26], the effective wellbore permeability value used in this analysis is many orders of magnitude higher compared to the most likely wellbore failure/degradation scenario (outside casing completion failure or degradation of the annulus, approximately 10^{-24} to 10^{-16} m^2).

Table 6 lists all 31 legacy wells locations, the mean cumulative CO_2 and brine leakages to the groundwater aquifer calculated at the end of the 50-year post-injection monitoring period, and their impact on the overlaying groundwater aquifer in terms of pH and TDS plume volume. The table lists CO_2 leakage amounts ranked from high to low.

Table 6. List of all 31 legacy well leakage and impact results to the groundwater aquifer at the end of the 50-year post-injection monitoring period.

X (m)	Y (m)	Well #	Total CO_2 Leakage (MT)	Total Brine Leakage (MT)	pH Plume (m^3)	TDS Plume (m^3)
319,407.1	4,016,070	15	6.30×10^{-4}	8.66×10^{-5}	0	0
316,533.8	4,016,479	14	4.99×10^{-4}	8.56×10^{-5}	0	0
316,599.5	4,014,454	23	3.46×10^{-4}	7.64×10^{-5}	0	0
316,599.3	4,014,061	12	3.01×10^{-4}	9.03×10^{-5}	0	0
317,407.7	4,016,870	20	2.80×10^{-4}	9.21×10^{-5}	0	0
317,001.5	4,015,657	7	2.25×10^{-4}	7.43×10^{-5}	0	0
316,987.9	4,014,458	13	2.17×10^{-4}	7.46×10^{-5}	0	0
318,193.5	4,013,648	6	2.14×10^{-4}	7.93×10^{-5}	0	0
318,205.7	4,013,242	18	1.45×10^{-4}	8.22×10^{-5}	0	0
319,792.1	4,014,438	17	1.13×10^{-4}	8.13×10^{-5}	0	0
319,003.5	4,014,425	30	1.10×10^{-4}	7.42×10^{-5}	0	0
319,401	4,015,259	26	1.06×10^{-4}	8.39×10^{-5}	0	0
319,799.9	4,015,249	16	1.05×10^{-4}	8.25×10^{-5}	0	0
319,397.2	4,014,857	21	1.02×10^{-4}	7.91×10^{-5}	0	0
319,425.5	4,015,635	22	7.76×10^{-5}	7.94×10^{-5}	0	0
320,211.9	4,014,707	8	7.66×10^{-5}	7.27×10^{-5}	0	0
319,792.2	4,012,839	3	7.51×10^{-5}	7.01×10^{-5}	0	0
319,446.7	4,013,692	11	6.98×10^{-5}	7.98×10^{-5}	0	0
319,009.2	4,013,233	19	6.43×10^{-5}	7.18×10^{-5}	0	0
318,617.8	4,013,076	4	4.89×10^{-5}	6.93×10^{-5}	0	0
320,170.2	4,013,250	9	4.79×10^{-5}	7.23×10^{-5}	0	0
319,780.2	4,013,646	28	4.58×10^{-5}	6.97×10^{-5}	0	0

Table 6. *Cont.*

X (m)	Y (m)	Well #	Total CO_2 Leakage (MT)	Total Brine Leakage (MT)	pH Plume (m^3)	TDS Plume (m^3)
319,001.6	4,014,030	10	2.92×10^{-5}	6.80×10^{-5}	0	0
318,602	4,013,236	29	2.56×10^{-5}	7.01×10^{-5}	0	0
320,156.9	4,012,433	24	2.39×10^{-5}	7.05×10^{-5}	0	0
320,541.3	4,014,727	1	1.99×10^{-5}	7.00×10^{-5}	0	0
320,989.5	4,015,102	27	7.53×10^{-6}	6.83×10^{-5}	0	0
320,561.2	4,013,902	5	5.38×10^{-6}	6.76×10^{-5}	0	0
320,561.5	4,014,308	31	0.00	6.71×10^{-5}	0	0
320,553.4	4,013,520	25	0.00	6.71×10^{-5}	0	0
320,904.7	4,013,513	2	0.00	6.71×10^{-5}	0	0
		All 31 wells	4.01×10^{-3}	2.34×10^{-3}		

Analyzing leakage results of 31 legacy wells shows that Well #15 (see Figure 18 for well # labeled) has the highest cumulative CO_2 leakage amount at the end of the 50-year post-injection monitoring period, while three wells that are located at the site domain edge (Wells #2, 25, and 31) show zero CO_2 leakage. The CO_2 leakage amount extends in two orders of magnitude, from the lowest 5.38×10^{-6} MT to the highest 6.30×10^{-4} MT for the non-zero CO_2 leakage legacy wells.

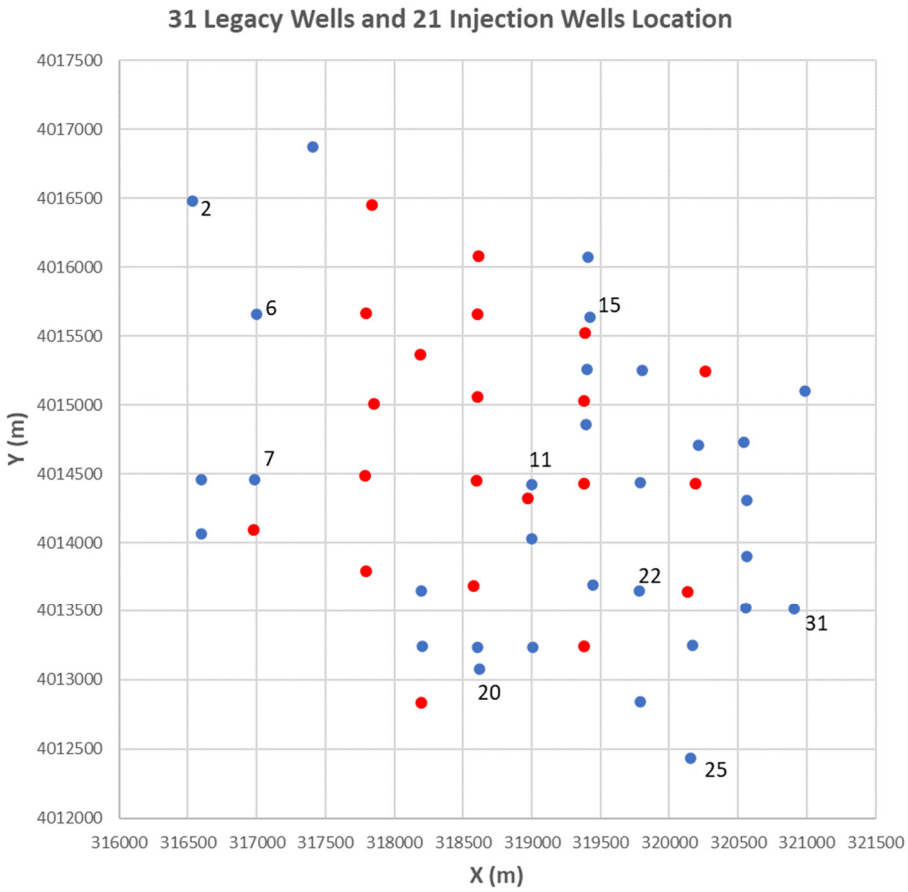

Figure 18. A total of 31 potential leakage legacy well locations (blue dots) and 21 CO_2 injection well locations (red dots). A few representative legacy wells are marked with well numbers.

A list of representative legacy wells is summarized in Table 7. Table 7 lists the representative legacy well's location, cumulative CO_2, and brine leakages to the groundwater aquifer at the end of the 50-year post-injection monitoring period, and also the relative distance of the legacy well from a nearby injection well (i.e., closer or far away from the nearby injection well).

Table 7. Representative legacy well's location, relative distance to nearby injection well, and cumulative CO_2 and brine leakage to groundwater aquifer at the end of the 50-year post-injection monitoring period.

Well #	Relative Distance to Nearby Injection Well	Distance (m) to Nearby Injection Well	Well Coordinate X (m)	Well Coordinate Y (m)	CO_2 Leakage (MT)	Brine Leakage (MT)
7	close	367	316,988	4,014,458	2.25×10^{-4}	7.43×10^{-5}
15	closer	121	319,426	4,015,635	6.30×10^{-4}	8.66×10^{-5}
11	closest	112	319,003	4,014,425	6.98×10^{-5}	7.98×10^{-5}
22	In the middle of Injection wells	360	319,780	4,013,646	7.76×10^{-5}	7.94×10^{-5}
31	far	775	320,905	4,013,513	0	6.71×10^{-5}
6	farther	801	317,001	4,015,657	2.14×10^{-4}	7.93×10^{-5}
2	farthest	1310	316,534	4,016,479	0	6.71×10^{-5}

Figure 14 shows the wellbore pressure time series for selected legacy wells. It shows Well #7 and Well #15 have higher wellbore pressure during the time period from year 10 to year 25, with Well #7 showing generally the highest pressure during this time period. Well #2 generally shows the lowest pressure.

Figure 15 shows that Well #15 displays much higher CO_2 saturation, Wells #6 and #7 show lower CO_2 saturation, Wells #11 and #22 show an order of magnitude lower CO_2 saturation compared to Well #15, and Well #2 shows zero CO_2 saturation.

Figure 19a,b show the temporal cumulative CO_2 and brine leakage to the groundwater aquifer from 31 legacy wells, respectively. Well #15 (grey colored line) displays the highest cumulative CO_2 leakage to the groundwater aquifer. Cumulative CO_2 leakage to the groundwater aquifer followed the same sequence in amount as CO_2 saturation.

Figures 20 and 21 show each legacy well's cumulative leakage amount relative to each other quantitatively in bubble plots (bigger bubble size corresponding to larger leakage). We can see that the wells with a higher CO_2 leakage amount (Figure 20) are located between 318,000 m and 320,000 m in the east-west direction and between 4,013,000 and 4,016,000 m in the north-south direction. There are more legacy wells in the FWU site located towards the eastern side of the domain, but the CO_2 leakage amount from these wells is relatively smaller.

Brine leakage amounts (Figure 21) are distributed relatively evenly among all legacy wells, with similar cumulative leakage amounts in the same order of magnitude for each well. Well #20 displays the highest brine leakage amount of 9.21×10^{-5} MT, and three near-site domain edge wells (#2, 25, and 31) display the lowest leakage amount of 6.71×10^{-5} MT.

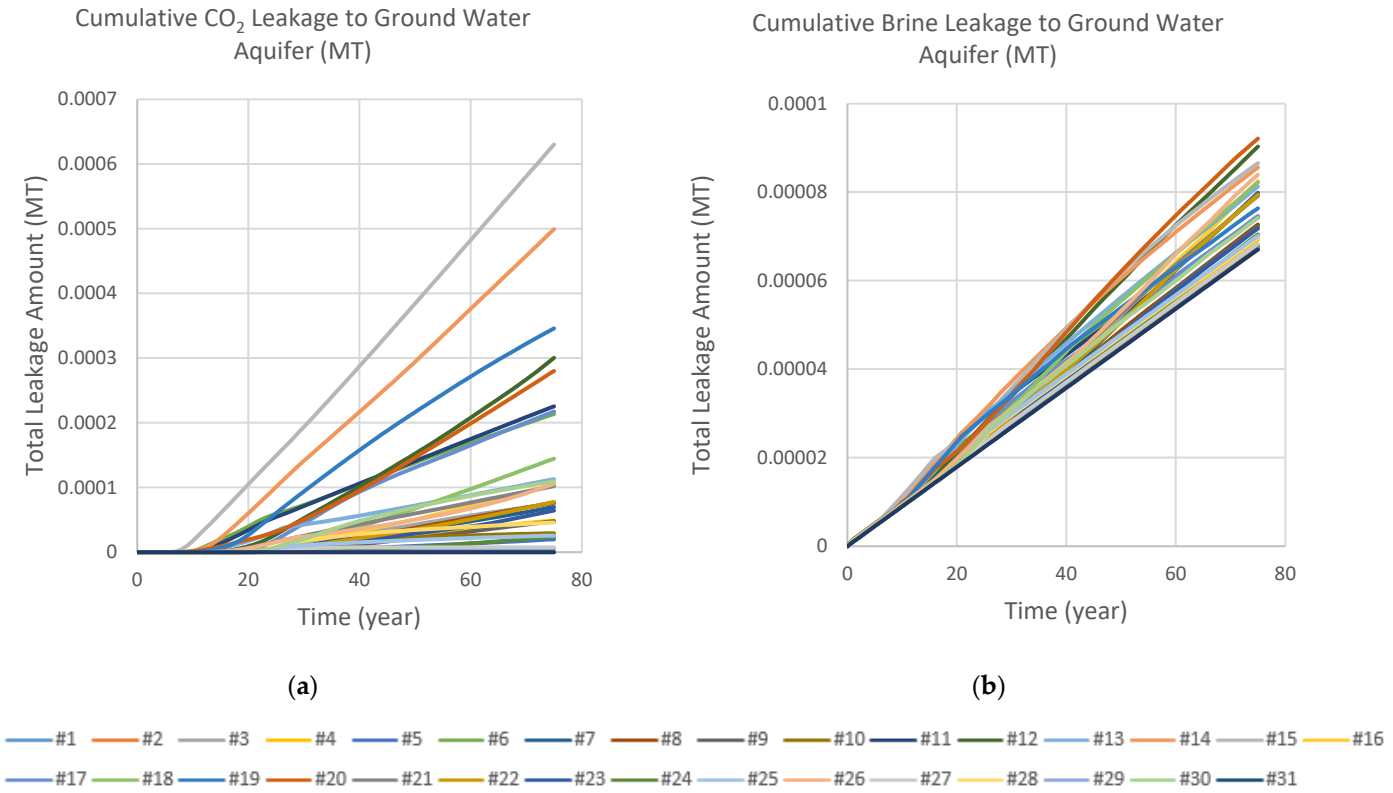

Figure 19. (**a**) Temporal cumulative CO_2 leakage to the groundwater aquifer for 31 legacy wells. (**b**) Temporal cumulative brine leakage to the groundwater aquifer for 31 legacy wells.

On individual well leakage analysis for a cemented wellbore scenario, multiple factors could affect the potential CO_2 and brine leakage risk, such as wellbore pressure, CO_2 saturation, the distance between a legacy well and a nearby injection well, and wellbore integrity condition. For example, Well #11 is a legacy well that is the closest to a nearby injection well, but it shows lower CO_2 leakage following the CO_2 saturation pattern. Well #15 shows the highest level of CO_2 saturation and leakage, but it has a lower wellbore pressure compared to Well #7 during the time period from years 10 to 25 (last 15 years of the injection period) and is not the closest legacy well to the nearby injection well. It seems that under the conservative assumption that all legacy wells have the same high effective permeability of 5×10^{-11} m^2, CO_2 saturation plumes impact wellbore CO_2 leakage the most, while reservoir pressure impacts brine leakage the most. All legacy wells leak brine in the same order of magnitude.

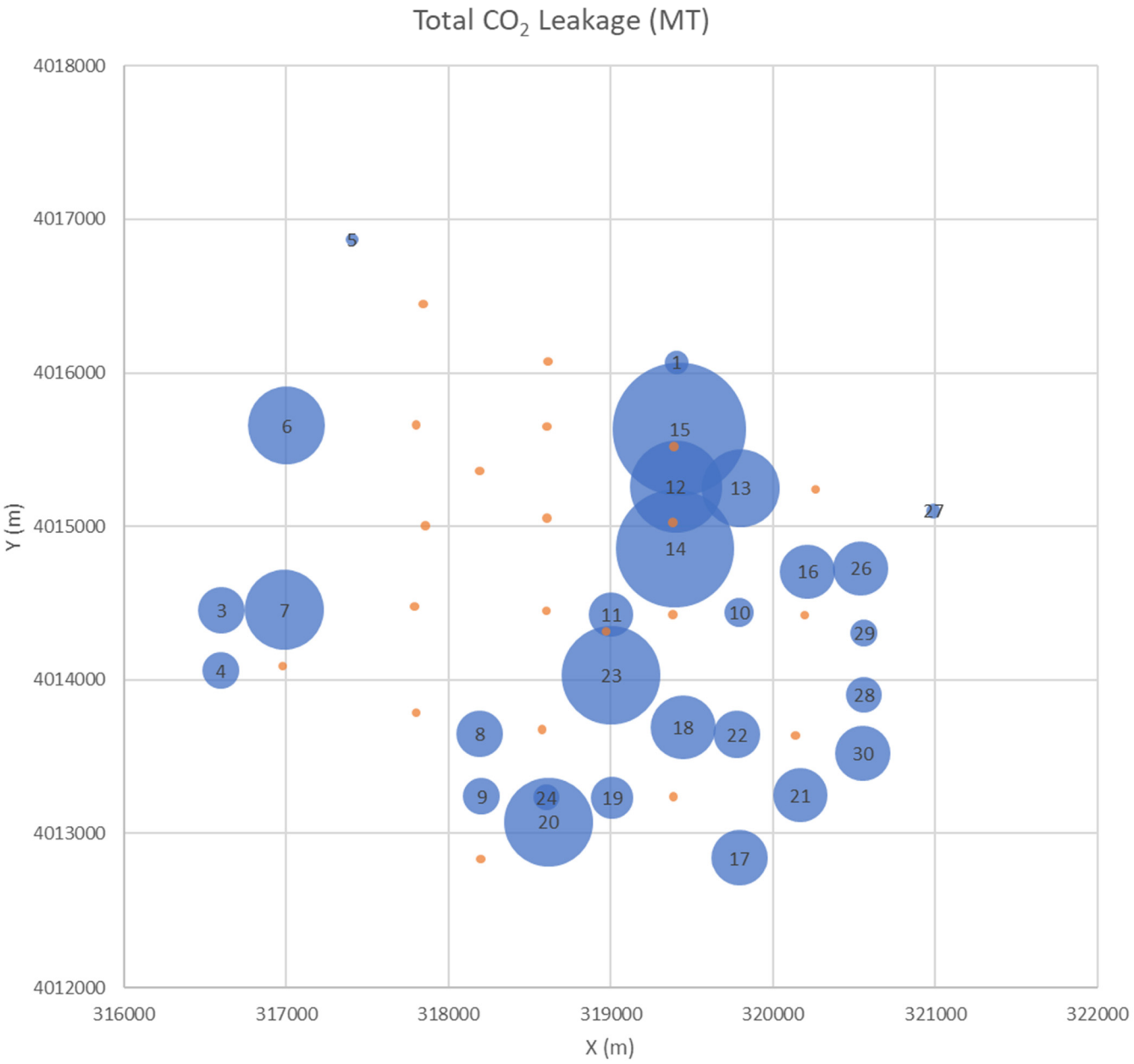

Figure 20. Relative view of CO_2 cumulative leakage amount for each legacy well at the end of the 50-year post-injection monitoring period. Bigger circle denotes higher leakage amount. (Note: background small orange dots shown are injection wells location).

Figure 21. Relative view of brine cumulative leakage amount for each legacy well at the end of the 50-year post-injection monitoring period. Bigger circle denotes higher leakage amount. (Note: background small orange dots shown are injection wells location).

4. Conclusions

To characterize the leakage potential of FWU wells, a workflow has been developed to import physics-based reservoir simulator (PETREL-ECLIPSE) pressure and CO_2 saturation results into the NRAP Integrated Assessment Model. NRAP tools, including NRAP-IAM-CS and RROM-Gen, are used to perform quantitative risk assessments of CO_2 and brine leakage. We applied NRAP tools for risk quantification of wellbore leakage that cover the full parameter range of ECLIPSE reservoir simulations at the Farnsworth Unit (FWU) Site and for various wellbore integrity distribution scenarios. Risk analysis of the leakage potential of FWU wells shows: Comparing the total amount of CO_2 injected, the highest cemented well integrity distribution scenario (FutureGen high flow rate) shows ~0.01% cumulative CO_2 leakage at the end of the 50-year post-injection monitoring period for a

25-year CO_2 injection duration; the highest possible leakage scenario (Open Well) shows ~0.1% cumulative CO_2 leakage.

To further analyze the leakage contribution from individual wells at the FWU site, two sets of NRAP simulations are carried out for leakage under different wellbore integrity conditions. For the open well scenario, compared to the total amount of CO_2 injected (about 10 million tons for each reservoir permutation scenario), the highest possible leakage scenario (open well) shows that Well #7 leaks the most with ~0.1% cumulative CO_2 leakage, and Well #15 has ~0.01% cumulative CO_2 leakage. All other legacy wells show no CO_2 leakage. For the cemented wellbore scenario, compared to the total amount of CO_2 injected (about 10 million tons for each reservoir permutation scenario), a conservative assessment with the highest effective wellbore permeability (5×10^{-11} m^2) shows that Well #15 leaks the most with ~0.0063% cumulative CO_2 leakage, and all 31 legacy wells show total ~0.04% cumulative CO_2 leakage at the end of the 50-year post-injection monitoring period. There is small brine leakage from each legacy well, with a total leakage amount of 2.34×10^{-3} MT for all 31 legacy wells. There is no impact on the groundwater aquifer in terms of pH and TDS.

This analysis is a highly conservative assessment, assuming all legacy wellbores fail/degrade at the same high effective permeability of 5×10^{-11} m^2. For the real situation at the FWU site, individual well leakage situations will be different based on each well's degradation status; more complete wellbore observational data will help facilitate the site-specific leakage risk assessment accurately.

Author Contributions: Conceptualization, H.V.; Formal analysis, S.C. and N.M.; Investigation, S.C. and N.M.; Methodology, all authors; Supervision, H.V.; Writing—original draft preparation, all authors; Writing—review and editing, all authors. All authors have read and agreed to the published version of the manuscript.

Funding: Funding for this project is provided by the U.S. Department of Energy's (DOE) National Energy Technology Laboratory (NETL) through the Southwest Regional Partnership on Carbon Sequestration (SWP) under Award No. DE-FC26-05NT42591.

Data Availability Statement: The numerical simulation model and results used as the basis for the leakage analysis were developed using the Eclipse® simulator are located on the Energy and Data eXchange (EDX) and available through the linked citations below at OSTI.gov. Moodie, Nathan. 2023. "BaseCase Model-No Capillary Pressure". United States. https://doi.org/10.18141/1997406. https://www.osti.gov/servlets/purl/1997406. Moodie, Nathan. 2023. "Morrow1 Model-No Capillary Pressure". United States. https://doi.org/10.18141/1997840. https://www.osti.gov/servlets/purl/1997840. Moodie, Nathan. 2023. "Morrow1 Model-with Capillary Pressure". United States. https://doi.org/10.18141/1997842. https://www.osti.gov/servlets/purl/1997842. Moodie, Nathan. 2020. "Linear Model 1-no Capillary Pressure". United States. https://doi.org/10.18141/1582040. https://www.osti.gov/servlets/purl/1582040. Moodie, Nathan. 2020. "Linear Model 1-with Capillary Pressure". United States. https://doi.org/10.18141/1582058. https://www.osti.gov/servlets/purl/1582058. Moodie, Nathan. 2023. "Hydrostratigraphic Region 4 Model-with HSU3-4Pc". United States. https://doi.org/10.18141/1997844. https://www.osti.gov/servlets/purl/1997844. Moodie, Nathan. 2023. "Hydrostratigraphic Region 4 Model-with HSU5 Capillary Pressure". United States. https://doi.org/10.18141/1997845. https://www.osti.gov/servlets/purl/1997845. Moodie, Nathan. 2023. "Hydrostratigraphic Region 4 Model-with HSU6 Capillary Pressure". United States. https://doi.org/10.18141/1997846. https://www.osti.gov/servlets/purl/1997846. Moodie, Nathan. 2023. "Hydrostratigraphic Region 4 Model-with HSU7-8 Capillary Pressure". United States. https://doi.org/10.18141/1997850. https://www.osti.gov/servlets/purl/1997850. Moodie, Nathan. 2023. "Hydrostratigraphic Region 1 Model". United States. https://doi.org/10.18141/1997851. https://www.osti.gov/servlets/purl/1997851. Moodie, Nathan. 2020. "Hydrostratigraphic Model 2-with Capillary Pressure". United States. https://doi.org/10.18141/1582039. https://www.osti.gov/servlets/purl/1582039. Moodie, Nathan. HydroStratigraphic Model 2-no Capillary Pressure. United States: N. p., 2020. Web. https://doi.org/10.18141/1582010. Moodie, Nathan. 2023. "Hydrostratigraphic Region 3 Model-with and without HSU Capillary Pressure". United States. https://doi.org/10.18141/1997854. https://www.osti.gov/servlets/purl/1997854. Moodie, Nathan. 2023.

"Hydrostratigraphic Region 4 Model-with HSUPc". United States. https://doi.org/10.18141/1997843. https://www.osti.gov/servlets/purl/1997843.

Conflicts of Interest: The authors declare no conflict of interest.

References

1. Haszeldine, R.S. Carbon Capture and Storage: How Green Can Black Be? *Science* **2009**, *325*, 1647–1652. [CrossRef] [PubMed]
2. Chen, S.; Liu, J.; Zhang, Q.; Teng, F.; McLellan, B.C. A critical review on deployment planning and risk analysis of carbon capture, utilization, and storage (CCUS) toward carbon neutrality. *Renew. Sustain. Energy Rev.* **2022**, *167*, 112537. [CrossRef]
3. Balch, R.; McPherson, B.; Grigg, R. Overview of a Large Scale Carbon Capture, Utilization, and Storage Demonstration Project in an Active Oil Field in Texas, USA. *Energy Procedia* **2017**, *114*, 5874–5887. [CrossRef]
4. Balch, R.; McPherson, B.; Will, R.A.; Ampomah, W. Recent Developments in Modeling: Farnsworth Texas, CO_2 EOR Carbon Sequestration Project. *SSRN Electron. J.* **2021**, 1–11. [CrossRef]
5. Balch, R.; McPherson, B. Associated Storage With Enhanced Oil Recovery: A Large-Scale Carbon Capture, Utilization, and Storage Demonstration in Farnsworth, Texas, USA. In *Geophysical Monitoring for Geologic Carbon Storage*; Huang, L., Ed.; John Wiley & Sons: Hoboken, NJ, USA, 2022; pp. 343–360. [CrossRef]
6. Wilson, E.J.; Friedmann, S.J.; Pollak, M.F. Research for Deployment: Incorporating Risk, Regulation, and Liability for Carbon Capture and Sequestration. *Environ. Sci. Technol.* **2007**, *41*, 5945–5952. [CrossRef] [PubMed]
7. White, S.; Carroll, S.; Chu, S.; Bacon, D.; Pawar, R.; Cumming, L.; Hawkins, J.; Kelley, M.; Demirkanli, I.; Middleton, R.; et al. A risk-based approach to evaluating the Area of Review and leakage risks at CO_2 storage sites. *Int. J. Greenh. Gas. Control* **2020**, *93*, 102884. [CrossRef]
8. Xiao, T.; McPherson, B.; Esser, R.; Jia, W.; Dai, Z.; Chu, S.; Pan, F.; Viswanathan, H. Chemical Impacts of Potential CO_2 and Brine Leakage on Groundwater Quality with Quantitative Risk Assessment: A Case Study of the Farnsworth Unit. *Energies* **2020**, *13*, 6574. [CrossRef]
9. Carroll, S.A.; Keating, E.; Mansoor, K.; Dai, Z.; Sun, Y.; Trainor-Guitton, W.; Brown, C.; Bacon, D. Key factors for determining groundwater impacts due to leakage from geologic carbon sequestration reservoirs. *Int. J. Greenh. Gas. Control* **2014**, *29*, 153–168. [CrossRef]
10. Onishi, T.; Nguyen, M.C.; Carey, J.W.; Will, B.; Zaluski, W.; Bowen, D.W.; Devault, B.C.; Duguid, A.; Zhou, Q.; Fairweather, S.H.; et al. Potential CO_2 and brine leakage through wellbore pathways for geologic CO_2 sequestration using the National Risk Assessment Partnership tools: Application to the Big Sky Regional Partnership. *Int. J. Greenh. Gas. Control* **2019**, *81*, 44–65. [CrossRef]
11. Bacon, D.H.; Qafoku, N.P.; Dai, Z.; Keating, E.H.; Brown, C.F. Modeling the impact of carbon dioxide leakage into an unconfined, oxidizing carbonate aquifer. *Int. J. Greenh. Gas. Control* **2016**, *44*, 290–299. [CrossRef]
12. Dilmore, R.; Wyatt, C.; Pawar, R.; Carroll, S.; Oldenburg, C.; Yonkofski, C.; Bacon, D.; King, S.; Lindner, E.; Bachmann, C.; et al. *NRAP Phase I Tool Development and Quality Assurance Process*; NRAP-TRS-II-021-2016; NRAP Technical Report Series; U.S. Department of Energy, National Energy Technology Laboratory: Morgantown, WV, USA, 2016; p. 64.
13. Pawar, R.J.; Bromhal, G.S.; Chu, S.; Dilmore, R.M.; Oldenburg, C.M.; Stauffer, P.H.; Zhang, Y.Q.; Guthrie, G.D. The National Risk Assessment Partnership's integrated assessment model for carbon storage: A tool to support decision making amidst uncertainty. *Int. J. Greenh. Gas. Control* **2016**, *52*, 175–189. [CrossRef]
14. Stauffer, P.H.; Viswanathan, H.S.; Pawar, R.J.; Guthrie, G.D. A system model for geologic sequestration of carbon dioxide. *Environ. Sci. Technol.* **2009**, *43*, 565–570. [CrossRef] [PubMed]
15. GoldSim Technology Group. *GoldSim Probabilistic Simulation Environment User's Guide*; Version 11.1.7; GoldSim Technology Group LLC: Issaquah, WA, USA, 2016; Volumes 1 and 2.
16. Czoski, P. Geologic Characterization of the Morrow B reservoir in Farnsworth Unit, TX Using 3D VSP Seismic, Seismic Attributes, and Well Logs. Master's Thesis, New Mexico Institute of Mining and Technology, Department of Earth and Environmental Science, Socorro, NM, USA, 2014; p. 102.
17. Ross-Coss, D.; Ampomah, W.; Balch, R.S.; Cather, M.; Mozely, P.; Rasmussen, L. An Improved Approach for Sandstone Reservoir Characterization. In Proceedings of the SPE Western Regional Meeting, Anchorage, AK, USA, 23–26 May 2016; SPE-180375.
18. Ampomah, W.; Balch, R.S.; Ross-Coss, D.; Hutton, A.; Cather, M.; Will, R.A. An Integrated Approach for Characterizing a Sandstone Reservoir in the Anadarko Basin. In Proceedings of the Offshore Technology Conference, Houston, TX, USA, 3 May 2016. [CrossRef]
19. Ampomah, W.; Balch, R.; Grigg, R.B.; Cather, M.; Gragg, E.; Will, R.A.; White, M.; Moodie, N.; Dai, Z. Performance assessment of CO_2-enhanced oil recovery and storage in the Morrow reservoir. *Geomech. Geophys. Geo-Energy Geo-Resour.* **2017**, *3*, 245–263. [CrossRef]
20. Gallagher, S.R. Depositional and Diagenetic Controls on Reservoir Heterogeneity: Upper Morrow Sandstone, Farnsworth Unit, Ochiltree County, Texas. Ph.D. Thesis, New Mexico Institute of Mining and Technology, Socorro, NM, USA, 2014.
21. Balch, R.; McPherson, B. Integrating Enhanced Oil Recovery and Carbon Capture and Storage Projects: A Case Study at Farnsworth Field, Texas. In Proceedings of the SPE Western Regional Meeting, Anchorage, AK, USA, 23–26 May 2016. [CrossRef]

22. Moodie, N.; Ampomah, W.; Jia, W.; Heath, J.; McPherson, B. Assignment and calibration of relative permeability by hydrostratigraphic units for multiphase flow analysis, case study: CO_2-EOR operations at the Farnsworth Unit, Texas. *Int. J. Greenh. Gas. Control* **2019**, *81*, 103–114. [CrossRef]
23. Moodie, N.; Ampomah, W.; Heath, J.; Jia, W.; McPherson, B. Quantitative analysis of the influence of capillary pressure on geologic carbon storage forecasts case study: CO_2-EOR in the Anadarko basin, Texas. *Int. J. Greenh. Gas. Control* **2021**, *109*, 103373. [CrossRef]
24. King, S. *Reservoir Reduced-Order Model—Generator (RROM-Gen) Tool User's Manual*; NRAP-TRS-III-0XX-2016; U.S. Department of Energy, National Energy Technology Laboratory: Morgantown, WV, USA, 2016.
25. Stauffer, P.; Chu, S.; Tauxe, C.; Pawar, R. *NRAP Integrated Assessment Model-Carbon Storage (NRAP-IAM-CS) Tool User's Manual Version: 2016.11-1.1*; NRAP-TRS-III-010-2016; NRAP Technical Report Series; U.S. Department of Energy, National Energy Technology Laboratory: Morgantown, WV, USA, 2016; p. 64. [CrossRef]
26. Carey, J.W. *Probability Distributions for Effective Permeability of Potentially Leaking Wells at CO_2 Sequestration Sites*; NRAPTRS-III-021-2017; NRAP Technical Report Series; U.S. Department of Energy, National Energy Technology Laboratory: Morgantown, WV, USA, 2017; p. 28.
27. Moodie, N.; Ampomah, W.; Jia, W.; McPherson, B. Relative Permeability: A Critical Parameter in Numerical Simulations of Multiphase Flow in Porous Media. *Energies* **2021**, *14*, 2370. [CrossRef]

Disclaimer/Publisher's Note: The statements, opinions and data contained in all publications are solely those of the individual author(s) and contributor(s) and not of MDPI and/or the editor(s). MDPI and/or the editor(s) disclaim responsibility for any injury to people or property resulting from any ideas, methods, instructions or products referred to in the content.